Memory Formalism, Nonlinear Techniques, and Kinetic Equation Approaches

V. M. Kenkre [1]

Consortium of the Americas for Interdisciplinary Science and the Department of Physics, University of New Mexico, Albuquerque, NM 87131

Abstract. Distinct applications of the tools of statistical mechanics to address several unconnected complex observations in interdisciplinary science are explained in four parts. The first deals with the memory function formalism and its application to varied topics: the origin of irreversibility, photosynthesis, sensitized luminescence, stress distribution in granular compacts, and magnetic resonance imaging. The second focuses on techniques of nonlinear equations applied to problems ranging from the Davydov soliton and the discrete nonlinear Schrödinger equation, to the propagation of epidemics and the Fisher equation. The third part discusses a few meeting places for the twin procedures of memory methods and nonlinear techniques. The fourth describes miscellaneous applications based on the Fokker-Planck and the Boltzmann equations to topics of current interest in ceramic science and condensed matter physics.

INTRODUCTION

The practitioner of statistical mechanics in modern times must possess the skills of a linguist, crossing over interdisciplinary barriers with the help of multiple vocabularies and techniques. Several such techniques are described in this article in the context of a number of diverse and unconnected phenomena. Two themes thread through the major part of this description: memory functions, and nonlinearity. What memory functions are good for, viz., the unification of coherent and incoherent transport, how they arise, e.g., from microscopic equations through the use of projection operators, and how they are utilized in often non-overlapping fields, e.g., in photosynthesis, stress distribution in granular compacts, or magnetic resonance imaging, are described in the first two sections. Nonlinear phenomena and the relevant techniques form the content of the next two sections where elliptic function solutions for the quantum nonlinear dimer are examined as well as the spread of epidemics and population dynamics of bacteria. Nonlinear equations with memory functions are treated next, with focus both on the competition and the coexistence of the two methods. Miscellaneous methods outside these two themes, particularly based on the Fokker-Planck and the Boltzmann equation, which have found use in recent investigations in ceramic science and condensed matter physics form the next section, and remarks conclude this article.

---

[1] E-mail address: kenkre@unm.edu.

CP658, *Modern Challenges in Statistical Mechanics: Patterns, Noise, and the Interplay of Nonlinearity and Complexity*, edited by V. M. Kenkre and K. Lindenberg

OSCILLATIONS VERSUS DECAYS: THE MEMORY FORMALISM

Background: why and how of Memory Functions

Among the bewildering variety of time evolutions found in the pursuit of statistical mechanics, two can be identified as extreme limits: oscillations, and decays. A mass attached to a spring, a planet circling a star, an ammonia molecule shuttling between two states, a Bose-Einstein condensate tunneling between two traps, and a Bloch electron in a pure crystal viewed in a localized representation all perform oscillations. All these systems, if or when affected by strong damping influences, exhibit decay in their evolution. The arrow of time, ever clear in macroscopic phenomena, presupposes decays. (For an exception, demonstrated by Alexandre Rosas at the PASI, see Fig. 1.) Reversible equations such as Newton's, Schrödinger's, or von Neumann's, accepted by most to underlie mechanical behavior, generally predict oscillations at the microscopic level. Irreversible equations such as the Boltzmann, Navier-Stokes or the Master equation, lead to approach to equilibrium, i.e., decays. One of the major problems of statistical mechanics, considered by some to be the central problem of the field, concerns the perhaps paradoxical coexistence of, and generally the relation between, microscopic short-time oscillations and macroscopic long-time decays. Furthermore, the study of that relation has practical relevance in many fields such as photosynthesis, electron conduction, and energy transfer. We begin by introducing the *memory function approach* which is eminently suited to investigate and describe this relation between oscillations and decays.

The simplest way to understand the power of the memory approach is by attempting with its help a unification of the evolution represented by

$$\frac{d^2y}{dt^2}+\omega^2 y=0 \tag{1}$$

which is reversible, oscillatory, and has trigonometric functions as solutions, with

$$\frac{dy}{dt}+\Gamma y=0 \tag{2}$$

which is irreversible, approaches equilibrium, and has an exponential as solution. Such unification is naturally performed by

$$\frac{dy(t)}{dt}+\Gamma\int_0^t ds\,\phi(t-s)\,y(s)=0 \tag{3}$$

via the "memory function" $\phi(t)$ which connects y at all times in the past to its derivative at the present. First, we note that (3) reduces to (2) and (1) in the respective extreme limits that the memory $\phi(t)$ is a δ -function, and that it is a constant (with the value ω^2/Γ). Second, if the memory is of neither extreme form but is intermediate,

$$\phi(t)=\alpha\exp(-\alpha t), \tag{4}$$

where the decay constant α equals ω^2/Γ, the evolution of y is that of (1) at times short with respect to $1/\alpha$ but of (2) at longer times. We thus see that the memory functions,

FIGURE 1. Ballistic motion with practically no damping, illustrated by a non-interacting Brazilian on the snowy slopes of El Catedral during the PASI.

by their very existence, can (i) unify oscillations and decays in extreme parameter limits (here, $\alpha \to 0$ and $\alpha \to \infty$), and (ii) provide an intermediate description for arbitrary α which is oscillatory at short times and decaying at long times (here, with respect to $1/\alpha$). It is of interest to note additionally that, if the memory is given by (4), differentiation of (3) yields the familiar equation for the damped harmonic oscillator:

$$\frac{d^2y}{dt^2} + \alpha \frac{dy(t)}{dt} + \omega^2 y = 0. \tag{5}$$

The combination of oscillatory and decaying behaviors as a function of time as well as of parameter ratios present in this elementary equation is well known.

Proceeding along identical lines, it is easy to see how memory functions unify *transport* which is coherent or wave-like as in the classical wave equation

$$\frac{\partial^2 P(x,t)}{\partial t^2} = v^2 \frac{\partial^2 P(x,t)}{\partial x^2} \tag{6}$$

which describes waves of a field P at a time t at position x which propagate with speed v, with its incoherent or diffusive counterpart characteristic of the classical diffusion (or Fourier's heat) equation

$$\frac{\partial P(x,t)}{\partial t} = D\frac{\partial^2 P(x,t)}{\partial x^2} \tag{7}$$

which predicts no waves at all but diffusive motion with a diffusion constant D. It is well known, for instance, that if you pluck a string in which the amplitude obeys the above respective equations, the disturbance would travel along the string without change of shape and with speed v in the former case while it slumps irreversibly spreading along the string in the latter case. These profoundly different kinds of transport are captured in one fell swoop by the memory function equation

$$\frac{\partial P(x,t)}{\partial t} = D\int_0^t ds\ \phi(t-s)\ \frac{\partial^2 P(x,s)}{\partial x^2}. \tag{8}$$

For instance, for the case of exponential memory (4) with $\alpha = v^2/D$, one obtains from (8) the telegrapher's equation

$$\frac{\partial^2 P(x,t)}{\partial t^2} + \alpha\frac{\partial P(x,t)}{\partial t} = v^2\frac{\partial^2 P(x,t)}{\partial x^2} \tag{9}$$

which, as is well-known, produces an intricate joining of wave-like propagation with diffusive evolution: in extreme parameter limits as well as in time for given parameter values. At short times, waves propagate but decay in time, and residual diffusive motion coexists in addition [1]. Indeed, for a localized initial condition, the mean square displacement defined as $< x^2 >= \int x^2 P(x,t)\,dx$ which is quadratic in t for the wave limit but linear in t for the diffusive limit, has the intermediate form

$$< x^2 >= 2D\left(t - \frac{1-e^{-\alpha t}}{\alpha}\right) \tag{10}$$

for the telegrapher's equation and passes smoothly from the quadratic form v^2t^2 to the linear form $2Dt$ (except for a constant term negligible by comparison at long times), as time increases from being smaller than, to larger than, $1/\alpha$.

The lesson learnt from these elementary considerations is that one might achieve much in the unification of the totally different limits of oscillatory and decaying time evolution, by focusing on memory functions. Is there a way of calculating memory functions for a given system from basic equations of motion such as the Schrödinger equation for a quantum system? We address this practical question via projection operator techniques next.

Projection Technique: Memories from Microscopics

The derivation of *macroscopic* equations of motion from the underlying *microscopics* is one of the central concerns of statistical mechanics [2]. Of the variety of procedures

and constructs such as the well-known BBGKY hierarchy that are met with in this context [3], one, the projection operator technique, leads naturally to memory functions. It was introduced originally [4] for the purpose of investigating the validity of the passage from the (microscopic) Schrödinger equation for the quantum mechanical amplitude of a system, equivalently the von Neumann equation for the density matrix ρ, given by

$$i\hbar\frac{d\rho}{dt} = [H,\rho] = L\rho, \tag{11}$$

where H is the Hamiltonian and L is the so-called Liouville operator, to the (macroscopic) Master equation for the probabilities P_ξ of occupation of states ξ, given by

$$\frac{dP_\xi}{dt} = \sum_{\xi'}\left[F_{\xi\,\xi'}P_{\xi'} - F_{\xi'\,\xi}P_\xi\right], \tag{12}$$

where the $F's$ are transition rates among the states. The projection method defines a linear, time-independent, idempotent operator $\mathscr{P}$ which, through its action on whichever operator it acts, extracts a part of that operator. This extracted part could be, for instance, the diagonal part of that operator in a given representation, or some generalization thereof. Application of $\mathscr{P}$ and of $1-\mathscr{P}$ successively to (11) yields (on putting $\hbar = 1$ for simplicity),

$$\begin{aligned}\frac{d\rho'}{dt} &= -i\mathscr{P}L\rho' - i\mathscr{P}L\rho'',\\ \frac{d\rho''}{dt} &= -i(1-\mathscr{P})L\rho'' - i(1-\mathscr{P})L\rho'.\end{aligned} \tag{13}$$

An exact formal solution of the second of these equations followed by a substitution in the former produces, perhaps surprisingly, a closed equation for ρ' alone, except for a formally known driving term in terms of the initial value of ρ'' :

$$\begin{aligned}\frac{d\rho'(t)}{dt} = -i\mathscr{P}L\rho'(t) - \mathscr{P}L\int_0^t e^{-i(t-s)(1-\mathscr{P})L}(1-\mathscr{P})L\rho'(s)\,ds\\ -i\mathscr{P}Le^{-it(1-\mathscr{P})L}\rho''(0)\end{aligned} \tag{14}$$

Notice the emergence of the memory in the middle term on the right hand side as is clear from the bridging that it performs between $\rho'(s)$ at past times s with the present time t. The last term is exactly zero if ρ'' is zero at the initial instant of time. Such a situation corresponds to what is called an 'initial random-phase approximation' unlike the '*repeated* random-phase approximation' shown by van Hove to be untenable [2]. The first term in the projected equation vanishes identically if the action of $\mathscr{P}$ involves diagonalization. In such cases, we have a closed memory-function evolution for ρ'. Although the expression for the memory appears complicated because of the tetradic operators, and although its precise nature will depend both on the system and the realization chosen for the projection operator, this technique [4] bypasses an enormous

amount of arduous calculation which characterizes other procedures employed for the same purpose [2]. It allows one to pass directly, in a certain sense effortlessly, from the microscopic von-Neumann equation (11) under certain conditions to an equation which, while not identical to the Master equation (12), has a striking resemblance to it:

$$\frac{dP_\xi(t)}{dt} = \int_0^t ds \sum_{\xi'} \left[\mathscr{W}_{\xi\,\xi'}(t-s) P_{\xi'}(s) - \mathscr{W}_{\xi'\,\xi}(t-s) P_\xi(s) \right]. \tag{15}$$

This so-called generalized master equation (GME) possesses memory precisely the way (3) and (8) do and is therefore able to describe coherent and incoherent transport in a unified manner. In appropriate limits it may tend to the Master equation (12) from which it differs in that the memory in the $\mathscr{W}$ functions in the GME is not generally short-lived as in the implied delta-function in (12). The GME (15), which made its first appearance only as a temporary step in the passage from microscopics to macroscopics, possesses all the powerful features of unification which its memory bestows upon it [5]. These features can been used in multiple ways in practical investigations [5, 6]. Recipes involving approximation procedures in some cases, and exact methods in others, can be developed to obtain the explicit forms of the $\mathscr{W}$ functions in terms of the Hamiltonian of the system in (11). This brief demonstration clarifies how the projection technique introduces memory functions and allows one to compute them, at least in principle. The intimate relationship of the projection technique and memory functions lies in the fact that $\mathscr{P}$'s project, i.e., contract the description; and generally, focusing on only a part of a system state produces memory function evolution, i.e., evolution non-local in time, for that contracted part. Of the many possible realizations of $\mathscr{P}$'s, let us mention one that diagonalizes an operator, thereby producing an evolution of the diagonal elements of the density matrix in a chosen basis, i.e., producing a Master equation for the probabilities as in (15),

$$< \xi | \mathscr{P} O | \mu > = < \xi | O | \xi > \delta_{\xi\,,\,\mu} \tag{16}$$

where O is any operator, ξ, μ are states of the system making up the chosen basis, and δ is the Kronecker delta; and one that coarse-grains and thermalizes in addition to diagonalizing, consequently producing an evolution of (coarse-grained) thermal probabilities of occupation of groups of states, producing a more appropriate Master equation for *macroscopic* probabilities,

$$< M, m | \mathscr{P} O | N, n > = \frac{e^{-\beta E_m}}{\sum_{m'} e^{-\beta E_{m'}}} \sum_{m''} < M, m'' | O | M, m'' > \delta_{m\,,\,n} \delta_{M\,,\,N} \tag{17}$$

where β is $1/kT$, the reciprocal of the product of the Boltzmann constant and the temperature, and E_m are energies of states m over which the coarse-graining (along with thermalization) is performed. The result of the coarse-graining is evolution in the probabilities of occupation of groups of states denoted by M. We refer the reader elsewhere [5, 6] for detailed derivations but point out here that M could, for instance, be the state of an electron (say a Wannier state centered around one lattice site in a band) while the m's could refer to phonon states over which one often wishes to coarse-grain the description.

The problem of the passage from reversible microscopics to irreversible macroscopics is understood rather simply through the use of GME's obtained with the help of projection operators which employ coarse-graining as in (17). The memory functions then have the form of Fourier transforms of entities, denoted by $Y(\omega)$, which are products of interaction matrix elements and density of states of the system [5]:

$$\mathscr{W}(t) = \int d\omega Y(\omega) cos(\omega t). \tag{18}$$

Appropriate behavior of these entities $Y(\omega)$ in the energy (or frequency) space results in the decay of the memory functions in time, when the thermodynamic limit is taken. The thermodynamic limit eliminates Poincaré cycles. The width of $Y(\omega)$ in ω-space is related reciprocally to the decay time of the memories $\mathscr{W}(t)$. Sharp peaks in $Y(\omega)$, arising either from sharp peaks in the density of states or in interaction matrix elements, result in long-lived memories. A large width of $Y(\omega)$ corresponds to sharp decay of the memory in time. The decaying memory functions describe reversible (or coherent) behavior at times short with respect to the decay times of the memories and irreversible (or incoherent) behavior at times long with respect to them. The philosophical requirements that the onset of irreversibility should depend on the system properties, that it should stem from looking at the system at a sufficiently coarse level, that it not occur for too small a system, and that it be valid only at sufficiently long times compared to microscopic times, are all fulfilled smoothly by this description without invoking abstruse arguments. A simple but satisfactory understanding of the reversibility-irreversibility problem in statistical mechanics is provided naturally, in this way, by the memory formalism (see the Appendix 'Poor Man's Version of the Origin of Irreversibility' in [5] for further details.)

The memory formalism is particularly useful in practical contexts. Two examples of memory functions derived for quantum mechanical systems follow, one obtained exactly and one perturbatively. Consider an electron or other (single-band) quantum particle moving via translationally invariant interaction matrix elements V_{mn} among the sites m,n of a $1-$dimensional lattice with periodic boundary conditions, and obeying (again we put $\hbar = 1$ for simplicity)

$$i\frac{dc_m}{dt} = \sum_n V_{mn} c_n. \tag{19}$$

Using no coarse-graining, and following the diagonalization definition (16) of the projection operator, it is possible to show [6] that the Laplace transform of the memory function $W_{mn}(t)$ is given by

$$\widetilde{\mathscr{W}_{mn}}(\varepsilon) = -\sum_k \left\{ \frac{e^{-ik(m-n)}}{\sum_q \left[\varepsilon + i\left(V^{k+q} - V^q\right)^{-1}\right]} \right\} \tag{20}$$

where k,q are reciprocal lattice vectors, and V^k is the Fourier transform $\sum_{(m-n)} V_{mn} e^{ik(m-n)}$. Indeed, it is possible to invert this Laplace transform and show that, for an infinite lattice and nearest neighbor V's, $V_{mn} = V(\delta_{m,n+1} + \delta_{m,n-1})$, the memory functions in the resulting GME for the probabilities $P_m = |c_m|^2$, which is merely (15) with $\xi = m$ and

$\xi' = n$, are

$$\frac{dP_m(t)}{dt} = \int_0^t ds \sum_n \left[\mathscr{W}_{mn}(t-s) P_n(s) - \mathscr{W}_{nm}(t-s) P_m(s) \right] \tag{21}$$

are given by

$$\mathscr{W}_{mn}(t) = \frac{1}{t} \frac{d}{dt} J^2_{m-n}(2Vt) \tag{22}$$

where the J's are ordinary Bessel functions [6, 7].

A second example, obtained perturbatively, has to do with the motion of an excitation moving between the two sites of a dimer (a $2-$site system) via matrix element V while at the same time interacting very strongly with vibrations. The Hamiltonian is

$$H = V\left(|1\rangle\langle 2| + |2\rangle\langle 1|\right) + \sum_q \omega_q b_q^\dagger b_q + \left(|1\rangle\langle 1| - |2\rangle\langle 2|\right) \sum_q g_q \omega_q \left(b_q + b_{-q}^\dagger\right) \tag{23}$$

in standard notation. The kets and bras describe the sites, and the b's are the second quantized phonon operators associated with the vibrations of mode q with frequencies ω_q and coupling constants g_q. Projection operators of the type of (17) which coarse-grain and thermalize over phonons, lead through a perturbative treatment [6, 8], to

$$\frac{dp(t)}{dt} + 2\int_0^t \mathscr{W}(t-s)\, p(s)\, ds = 0 \tag{24}$$

for the probability difference $p(t)$ of the excitation occupation of the two sites. The memory function is given generally by

$$\mathscr{W}(t) = 2V^2 e^{h(t)-h(0)} + c.c. \tag{25}$$

$$h(t) = 2\sum_q g_q^2 \left[n_q e^{i\omega_q t} + \left(n_q + 1\right) e^{-i\omega_q t} \right]. \tag{26}$$

Here n_q is the Bose factor $\left(e^{\beta\omega_q} - 1\right)^{-1}$. For the case of zero temperature and a single mode of vibration, the memory reduces to

$$\mathscr{W}(t) = 2V^2 e^{-2g^2(1-\cos\omega t)} \cos\left(2g^2 \sin\omega t\right) \tag{27}$$

Although simple in form, this memory function is rich in content. Much can be learnt about the dynamics of the dimer from a mere inspection of the memory [9] and the interplay of its several characteristic time constants, for instance, $1/\omega$, $1/g\omega$, and $1/g^2\omega$.

The generalized form this memory function takes at finite temperatures and multiple vibrational modes does not seem to be widely known. In the case appropriate to optical phonons centered around frequency ω with a narrow width σ, it can be written down as

$$\mathscr{W}(t) = 2V^2 e^{-2g^2 \coth(\omega/2kT)(1-\zeta(t)\cos\omega t)} \cos\left(2g^2 \zeta(t) \sin\omega t\right) \tag{28}$$

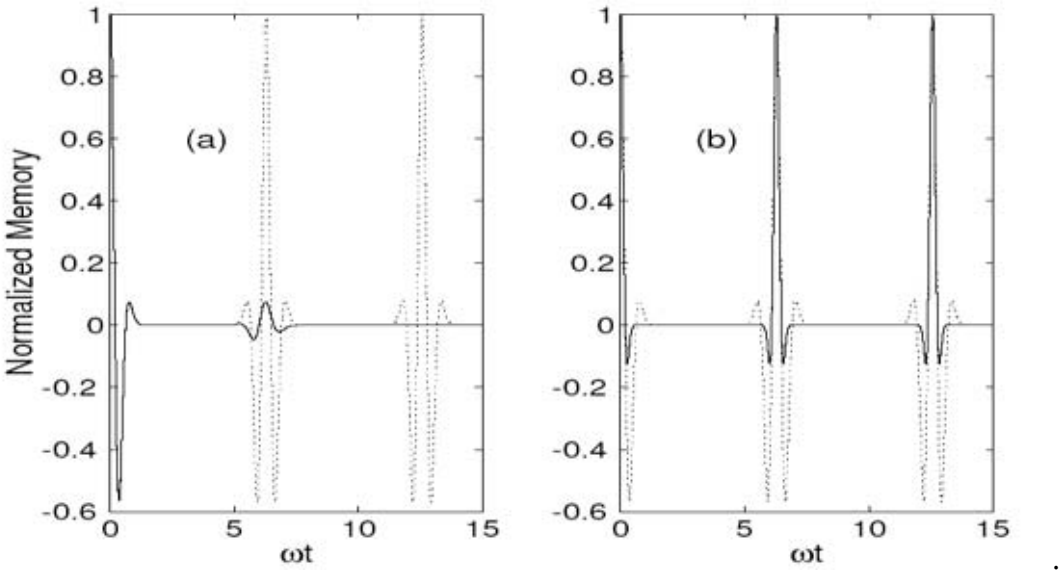

FIGURE 2. Normalized memory function $\mathscr{W}(t)$ from (27) and (28) for a quantum quasiparticle moving between two dimer sites while interacting strongly with vibrations, plotted as a function of the dimensionless time ωt. Parameter values are arbitrary: $g = 2$ in both (a) and (b), $\sigma = 0.1$ in (a), and $\omega/2kT$ equals 0.2 in the solid line of (b). The dotted line is the single-mode zero-temperature prediction of (27).

where $\zeta(t)$ is the Fourier transform of the phonon density of states, typified by a Gaussian $exp(-\sigma^2 t^2)$. The general memory reduces to the single-mode zero-temperature expression (27) in the appropriate limit. We show in Fig. 2 a plot of (28), for arbitrary values of the parameters. The dotted line in both (a) and (b) is the zero-temperature single-mode version in (27) and exhibits 'silent runs' followed by full recurrences, repeated decays (of the envelope), and fast oscillations within the envelope, on the three respective time scales. The recurrences do not occur fully in the solid line in (a) which describes the effect of multiple modes represented by a finite frequency width $\sigma/\omega = 0.1$: the maximum value of the memory function decays strongly from one recurrence to the next. The temperature is taken to be zero in (a). In (b) we display the effect of finite temperature. The solid line corresponds to $2kT/\omega = 5$ while the dotted line is the zero-temperature case, σ being zero in both cases in (b). We see that the oscillations to negative values are substantially suppressed at non-zero temperatures.

The second of the three characteristic inverse times mentioned above for the zero-temperature case (27) as being $g\omega$, and best looked upon as the geometric mean of the polaronic binding energy $g^2\omega$ and the phonon energy ω (we have put $\hbar = 1$ in all these considerations), is, in the general case (28), equal to $g\omega\sqrt{\coth(\omega/kT)}$. As $T \to 0$, when the coth saturates to 1, we get back the earlier form, but for large T, the second of the three characteristic inverse times is the geometric mean of $g^2\omega$ and the thermal energy $2kT$. Considerable insights into dynamics may be obtained thus through a direct inspection of the memory functions. We remark in passing that a simple relation exists [9] between the memory description via (28) and the so-called 'non-interacting blip approximation' [10] introduced in the analysis of the spin-boson problem.

APPLICATIONS OF THE MEMORY FORMALISM

Applications of the memory formalism abound. We mention illustrations from three areas selected because they are rather unrelated to one another: photosynthesis and sensitized luminescence, nuclear magnetic resonance probes of confined motion, and stress distribution in granular compacts. Through this selection, we illustrate the enormous breadth of applicability of the formalism.

Photosynthesis and Sensitized Luminescence

The study of the biological process of photosynthesis is important and intriguing: important in that understanding it might save mankind from starvation when food resources run out, and intriguing because of the complex physical processes underlying it, including energy transfer. Much work has been directed at the understanding of the energy transfer that occurs in photosynthetic systems as the electronic excitation created by absorption of sunlight travels from whatever location it lands at, to the reaction centers where it is caught and used to cook carbon dioxide and water into sugar. The nature of the transport of excitation, in particular whether it proceeds coherently or incoherently, has been an active goal of investigations. One application of the memory formalism is a unification of coherent and incoherent transfer rates carried out [11] simply on the basis of the mean square displacement formula (10). Another illustrates coherence effects on the quantum yield observed in sensitized luminescence experiments in molecular crystals [6]. Here we will briefly touch upon a third application which addresses the calculation of realistic memories directly from optical spectra [12].

Equation (18) shows that the memory $\mathscr{W}(t)$ is intimately tied to the quantity $Y(\omega)$, and that the latter is determined by the transfer interaction matrix elements and the density of states. The transfer of excitations in photosynthetic systems proceeds primarily via dipole-dipole interactions [13]. A close relation exists between optical spectra of the molecules in the photosynthetic unit, and transfer rates in an ordinary Master equation such as (12) describing excitation transfer. In order to address the issue of how coherent the transfer is, it is possible to employ the GME (15) instead of (12), and to calculate its memory directly from the optical spectra. Förster's well-known prescription [13] to calculate Master equation rates F_{mn} from spectra obtains them from the overlap of the spectra:

$$F_{mn} = const. \frac{1}{R_{mn}^6} \int_0^\infty d\omega \, \frac{A(\omega) E(\omega)}{\omega^4}. \tag{29}$$

The constant of proportionality is unimportant for the present discussion. The inverse dependence on the 6th power of the intermolecular distance R_{mn} between the donor and acceptor molecules at sites m and n is characteristic of the dipole-dipole interaction, and A and E are the absorption spectrum of the acceptor, and the emission spectrum of the donor, respectively.

The generalized prescription to obtain memories $\mathscr{W}_{mn}(t)$ consists of calculating the overlap indicated in (29) after displacing the modified spectra relative to each other on the frequency axis by an amount z for all possible values of z from $-\infty$ to $+\infty$, and

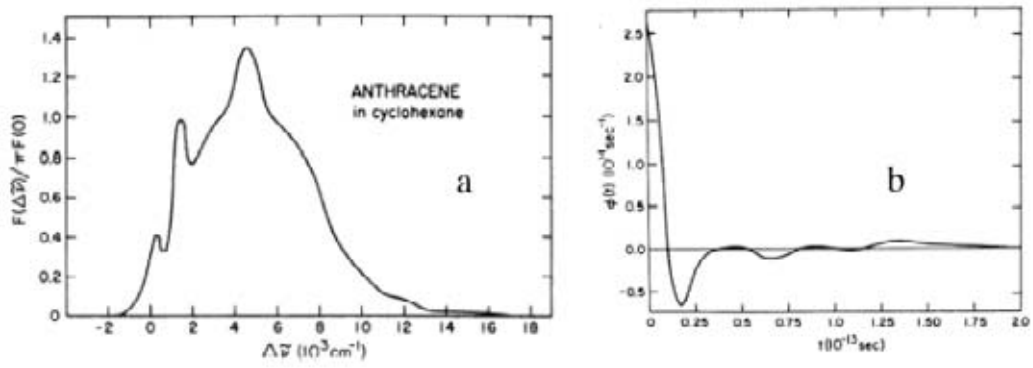

FIGURE 3. The prescription (30) to obtain memories from spectra illustrated for anthracene in cyclohexane solution at room temperature: (a) shape of the extended overlap integral as a function of the displacement z termed in the figure $\Delta\widetilde{\nu}$ and (b) memory function $\mathscr{W}(t)$ termed in the figure $\phi(t)$ as a function of time obtained through a Fourier transform of the dependence in (a). See [12].

then Fourier-transforming the $z-$dependence of the overlap thus obtained. The resulting expression [12],

$$\mathscr{W}_{mn}(t) = const.\frac{1}{R_{mn}^6}\int_{z=-\infty}^{z=+\infty} dz\,\cos(zt)\int_0^{\infty} d\omega\,\frac{A(\omega-z)\,E(\omega+z)}{(\omega-z)^3(\omega+z)}, \qquad (30)$$

wherein the proportionality constant differs from that in (29) by a factor of π, can be used directly for coherence investigation purposes. We display in Fig. 3 the spectra in (a) and the memory in (b) for anthracene in cyclohexane solution[2] . Notice that (30) is precisely of the form (18) discussed above in the context of the origin of irreversibility. These considerations are of practical importance not only in photosynthesis but also in the more general subject of sensitized luminescence in molecular crystals and aggregates [6] as well as in more modern observational contexts such as transient gratings [6, 14]. Cited references should be consulted for further detail.

NMR Probes of Confined Motion

Nuclear magnetic resonance probes of confined spaces, as in porous rock or capillaries in the human body, are of great current importance in the industry and in medicine. The basic idea underlying the NMR probe is to monitor the spin dynamics of protons associated with water molecules, in the presence of a static (gradient) magnetic field. The latter systematically changes the precession frequency of the spins in space. Observations of the spin echo kind allow one to gather information regarding the diffusion of the spins [15]. The diffusion is affected by the walls of the confined spaces. It is

[2] Although the presence of inhomogeneous broadening in these spectra may raise issues about the detailed applicability of the available spectra in this prescription, the example makes clear the procedure.

thus possible to collect information about such properties as the connectivity of space inside the confined regions. The theoretical interpretation of the observations is based on the Torrey-Bloch equation [16] which describes the evolution of $\rho(r,t)$, the space-dependent density matrix of the spin at position r and time t. This evolution is in part quantum mechanical, in that it describes the spin dynamics, and in part classical, in that it describes spatial diffusion. Written for the magnetization $M(r,t)$ instead of for $\rho(r,t)$, the Torrey-Bloch equation is

$$\frac{\partial M(r,t)}{\partial t} = -i\gamma g x f(t) M(r,t) + D\nabla^2 M(r,t), \tag{31}$$

where g is the strength and $f(t)$ the time dependence of the applied gradient magnetic field, γ is the gyromagnetic ratio, and D is the diffusion constant. The observable of interest is the total magnetization integrated over all space: $M(t) = \int M(r,t)\, dr$.

Projection techniques and resulting memory functions find excellent employment here [17]. The definition of a projection operator $\mathscr{P}$ whose essence is to integrate over all space whatever it operates on,

$$\mathscr{P} O(r,t) = \sigma(r,0) \int O(r')\, dr', \tag{32}$$

where $\sigma(r,0)$ describes the initial distribution of spins, allows one to obtain a memory-function equation for the total magnetization:

$$\frac{dM(t)}{dt} + f(t) \int_0^t f(t')\, \phi(t-t')\, M(t') = 0. \tag{33}$$

The memory function $\phi(t)$ can be shown in the weak-coupling approximation to be proportional to the classical autocorrelation function of the displacement of the diffusing spin. Restricting our analysis to a 1-dimensional system, we can write

$$\phi(t) = \gamma^2 g^2 \langle x x(t) \rangle. \tag{34}$$

Standard manipulations with the diffusion equation result in an infinite series expression for $\langle x x(t) \rangle$. If the diffusing spin is confined to a finite segment of length a,

$$\langle x x(t) \rangle = \frac{8a^2}{\pi^4} \sum_{n=1}^{\infty} \frac{1}{(2n-1)^4} \exp\left[-\frac{(2n-1)^2 \pi^2 D t}{a^2} \right]. \tag{35}$$

It has been shown [17] that, independently of the values of the physical parameters, this expression for $\langle x x(t) \rangle$ can be represented by a single exponential to an excellent approximation, and that the memory is, then,

$$\phi(t) = C^2 e^{-2\lambda t}. \tag{36}$$

Here C is $(\gamma g a)^2/12$ and $\lambda = 5D/a^2$. This memory-function description leads to the explicit prediction that, even for a time-independent applied gradient field, i.e., if $f(t)$

is a constant, the signal represented by $M(t)$ can exhibit oscillations in time, provided the ratio C/λ is large enough. The quantity C/λ is, except for a numerical constant, the ratio of the extreme difference between the precessional frequencies of the spin in the confining space, viz., γga, to the reciprocal of the time it would take the spin to diffuse from one end of the confining segment to the other, viz., D/a^2. The prediction of this memory description that oscillations will occur for large enough gradient field strength, or for small enough diffusion constant, are borne out by experiment. By contrast, other calculational approaches, for instance the frequently used cumulant expansion technique [18], are unable to predict such oscillations [17].

Stress Distribution in Granular Compacts

An unexpected application of the memory formalism crops up in the field of stress distribution in granular compacts [19–21]. The behavior of granular materials [22] under compressive stresses is poorly understood, despite more than a century of research in civil engineering under the topic of soil mechanics, in mechanical, ceramic, and metallurgical engineering in the context of the pressing and sintering processes; and in geodynamics such as in the study of earthquakes and avalanches. A key observation reported [23, 24] in the study of granular compacts is stress oscillations in *space* (not in time). A theoretical framework has been constructed [19] to address such observations on the basis of the idea of the formal interpretation of the vertical spatial coordinate as time [19, 25]. A variety of different starting points, stress balance equations and phenomenological constitutive equations in one case [19], effective medium approximations in another [20], and the use of stochastic considerations in yet another [21], have led to the demonstration that a plausible equation governing $\sigma_{zz}(x,y,z)$, the diagonal $z-$component of the stress tensor, where z is the vertical direction or the direction along which external stress is applied, is the memory equation

$$\frac{\partial \sigma_{zz}(x,y,z)}{\partial z} = D\int_0^z dz'\,\phi(z-z')\,\nabla^2\sigma_{zz}\left(x,y,z'\right). \tag{37}$$

Properties of the granular material are reflected in $\phi(z)$ and D.

The 'memory' in this formalism is not temporal, but spatial. The formalism provides a unification of two seemingly unrelated treatments of stress distribution available in the literature: a wave-like treatment [25] which might apply to a granular system consisting of identical, frictionless spherical particles arrayed in a perfectly ordered lattice, and a diffusion-like analysis [26] in which the transmitted stress is described as arising from a sum of contributions from random probabilistic transmission of forces from particles in one layer of the granular material to particles in the next lower layer.

Application [19] of the memory formalism to the analysis of stress distribution in unbounded media may be illustrated by taking the applied stress $\sigma_{zz}(x,0)$ at the 'surface' $z=0$ to be a delta function $\delta(x)$. If the memory is assumed exponential for simplicity, i.e., if $\phi(z)=c^2\exp(-\alpha z)$, the stress is found to be

$$\sigma_{zz}(x,z) = e^{-\alpha z/2}\left[\frac{\delta(x+cz)+\delta(x-cz)}{2}+T\right], \tag{38}$$

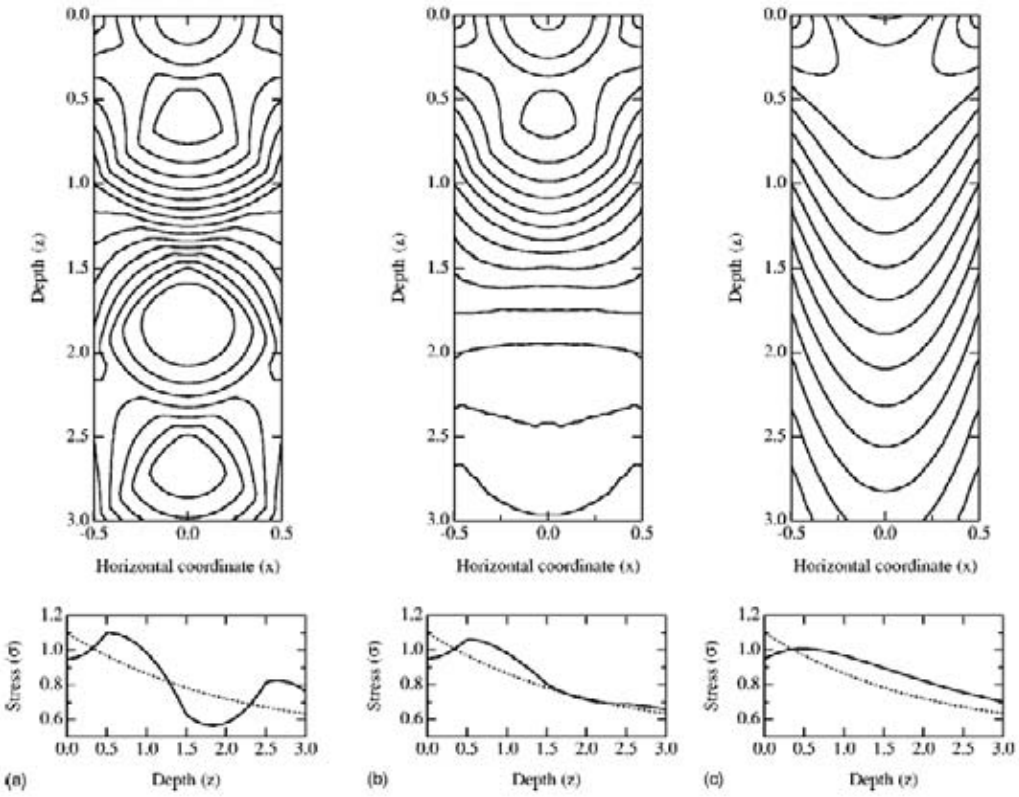

FIGURE 4. Memory description of stress distribution in a granular compact showing the presence in some samples and the absence in others of stress oscillations with depth within the compact. The upper frames are contour plots of the stress while the lower frames show oscillations with depth explicitly. Units are arbitrary. Value of the decay constant α of the memory, consequently its incoherence and diffusive behavior, increases from (a) through (c).

where the term T vanishes identically for $cz \leq x$, and equals, for $cz \geq x$,

$$T = \left(\frac{\alpha}{4c}\right)\left\{I_0\left(\frac{\alpha}{2c}\sqrt{c^2z^2 - x^2}\right) + \frac{cz}{\sqrt{c^2z^2 - x^2}} I_1\left(\frac{\alpha}{2c}\sqrt{c^2z^2 - x^2}\right)\right\}, \qquad (39)$$

the I's being modified Bessel functions. The so-called phenomenon of 'light cones' mentioned in [25] is recovered in the limit $\alpha = 0$. Diffusive stress propagation with its characteristic Gaussian profile is recovered in the opposite limit.

Stress distribution in laterally *bounded* media, such as pipes and compacts, has also been addressed satisfactorily with the help of this memory formalism [19]. The basic calculational step is the solution of a partial differential equation with mixed boundary conditions at the walls. Observed [23, 24] oscillations of stress emerge naturally. For want of space we only display one of these results pictorially (see Fig. (4)) and refer the reader to the original articles for the analysis.

NONLINEAR TECHNIQUES: QUASIPARTICLES, MICE, AND BACTERIA

As we pass from the memory formalism to techniques based on nonlinear equations in this section, we lose the support of powerful, universally applicable, procedures of linear mathematics based on superposition, such as Laplace and Fourier transforms, but gain remarkable features such as threshold phenomena and abrupt transitions. We analyze these phenomena for two quite disparate kinds of systems: microscopic quasiparticles such as electrons interacting with vibrational excitations or Bose-Einstein condensates obeying the discrete nonlinear Schrödinger equation in condensed matter, and macroscopic entities such as moving mammals or growing bacteria obeying Fisher-like equations in the ecological/biological contexts of the spread of epidemics or of infections in surgical wounds.

Quasiparticles and Elliptic Functions

If the amplitude c_m of a quantum particle, e.g., an electron or exciton, to be at a site m obeys (19) augmented by a nonlinear term [27],

$$i\frac{dc_m}{dt} = \sum_n V_{mn}c_n - \chi|c_m|^2 c_m, \tag{40}$$

the transport of the particle changes drastically [28, 29] as the nonlinearity parameter χ is varied with respect to the interaction matrix elements V_{mn}. The physics behind the nonlinear term has been often assumed to be that the site energy of the particle is lowered as a result of strong interactions with vibrations, whenever the site is occupied by the particle. Equation (40) is known as the discrete nonlinear Schrödinger equation (DNLSE). Doubts have been cast on the derivation of the DNLSE from quantum mechanics in this polaron context [30–33]. More recently, (40) has reappeared in new guise as the Gross-Pitaevskii equation in Bose-Einstein condensate tunneling [34–36]. In that setting, it is not vulnerable to the objections raised to its derivation for polaron dynamics. The insights gathered from the equation in the polaron field [28, 29] are being reused [35, 36] in the Bose-Einstein context.

Much can be understood within a two-site system, i.e., when m,n in (40) take on values $1,2$ only. Conversion of (40) into a density matrix equation, followed by focusing on the probability difference $p = |c_1|^2 - |c_2|^2$, leads to

$$\frac{d^2p}{dt^2} = Ap - Bp^3, \tag{41}$$

where A and B are given in terms of the system parameters as well as the initial conditions of the system:

$$\begin{aligned} A &= \left(\chi^2/2\right)p_0^2 - 4V^2 - 2V\chi\left(\rho_{12}+\rho_{21}\right)_0, \\ B &= \chi^2/2. \end{aligned} \tag{42}$$

The suffix 0 denotes the initial values, and ρ_{12} and ρ_{21} are site-offdiagonal matrix elements of the density matrix. The probability difference p between the sites can be solved exactly in terms of Jacobian elliptic functions. Solutions for arbitrary initial conditions will be found elsewhere [37]. For a *localized* initial condition, wherein the quasiparticle occupies one of the two sites initially, p is given by

$$\begin{aligned} p(t) &= cn(2Vt, \chi/4V) \ \ for\ \chi < 4V, \\ &= dn(\chi t/2, 4V/\chi) \ \ for\ \chi > 4V, \end{aligned} \tag{43}$$

showing oscillations on both sides of zero if the nonlinearity is small enough, and oscillations only on one side of zero, signifying selftrapping of the quasiparticle, if the nonlinearity χ exceeds $4V$. In (43), $\chi/4V$ is the elliptic modulus. The transition evolution occurs at $\chi = 4V$, i.e., when the elliptic modulus equals 1. At that point, $p(t)$ becomes the hyperbolic secant of $2Vt$, equivalently of $(1/2)\,\chi t$. The physical description is that, as the quasiparticle moves between sites, its site energy is repeatedly lowered at the site which it occupies. The energy mismatch, introduced by the very existence of the quasiparticle at one or the other of the sites, hinders the motion to an extent determined by the value of the nonlinearity χ relative to the transfer matrix element V. If the latter is large enough, the site energy returns to the unlowered value when the quasiparticle leaves the site and the motion, while slowed, is still fully oscillatory. This is the *cn* situation. If the nonlinearity χ is larger than the critical value $4V$, the lowered site energy cannot ever return to its value in the absence of the quasiparticle, and the particle is selftrapped. A lucid explanation of the phenomenon of selftrapping is provided with ease by the DNLSE.

We refer the reader to the extensive literature [38] that has gathered around descriptions of the nonlinear evolution described by the DNLSE, and point out here a generalized form of the equation which was constructed through a mixture of some rigorous, and some phenomenological, arguments:

$$\begin{aligned} i\hbar\frac{d\rho_{mn}}{dt} = [V,\rho]_{mn} - \chi\,(\rho_{mm} - \rho_{nn})\,\rho_{mn} - i\frac{\chi}{\Gamma}\rho_{mn}\,([V,\rho]_{mm} - [V,\rho]_{nn}) \\ -i\alpha\,(1-\delta_{mn})\,(\rho_{mn} - \rho^{eq}_{mn})\,. \end{aligned} \tag{44}$$

This equation, termed the 'ecumenical equation' [29], describes the evolution of the density matrix elements in the site representation in the presence of interactions with a thermal reservoir, and unifies a number of aspects of the nonlinear behavior of the quasiparticles. In addition to the intersite transfer matrix elements V_{mn} and the nonlinearity parameter χ present in (40), we have here Γ, α, and ρ^{eq}. The first describes the rate at which dissipation results in driving the vibrational part of the system to its slaved state so that it can be eliminated from consideration, in other words the rate at which the nonadiabatic process occurs [39]. The second describes the dephasing process [40] which drives the off-diagonal elements of the quasiparticle density matrix to their thermal values, ρ^{eq} being the thermal density matrix. The 'ecumenical equation' combines all these, motion, nonlinearity, nonadiabaticity, and thermalization into the single evolution (44), and predicts exceedingly interesting phenomena such as limit cycles and bifurcations [29, 41].

Of mice and men

At the macroscopic end of the application spectrum of nonlinear techniques, we consider two systems. The first is the spread of the hantavirus, a terrifying epidemic discovered in the last decade, transmitted from mouse to mouse, and passed on to human beings from the mice. The second is the evolution of bacteria in a Petri dish. We begin with considerations of the hantavirus [42, 43]. When infected by the hantavirus, the mice live happily ever after (having coexisted for millions of years with the virus), but humans much less so, if fortunate enough to live at all after being infected. Because the evolution of humans lies *on top of* that of the mice, meaning that no feedback effects are known from the human to the mice population, it is sufficient to consider the evolution of the mice alone. Appropriate description [44] is in terms of two classes of mice, susceptible and infected, represented by M_S and M_I respectively. Sex and age composition of the population are considered details and disregarded in this basic AK model:

$$\frac{\partial M_S}{\partial t} = bM - cM_S - \frac{MM_S}{K} - aM_IM_s + D\frac{\partial^2 M_S}{\partial x^2}, \tag{45}$$

$$\frac{\partial M_I}{\partial t} = -cM_I - \frac{MM_I}{K} + aM_IM_s + D\frac{\partial^2 M_I}{\partial x^2}. \tag{46}$$

Here c is the decay rate by natural death, a is the rate at which encounters of the two types of mice convert susceptible to infected, and D is the diffusion constant with which the mice move over the terrain, whether infected or susceptible. The resources (food, water, vegetation) are described by K which is generally time and space dependent: it is the primary control parameter in the AK analysis [3]. The effect of the terms containing K is to limit the growth of the populations at a rate proportional to the susceptible or infected mice population and also to the total population $M = M_S + M_I$ with which it competes for resources. Since infected mice are made, not born, the term bM which describes growth via birth, appears only in the M_S equation, and is proportional to the total mice population. We have written the single second spatial derivative in the last term in each of the (45) and (46) for simplicity. In a realistic situation we replace it by the Laplacian.

Steady-state analysis in the absence of diffusion shows [44] that a bifurcation phenomenon occurs according to whether the control parameter K is smaller or larger than a critical value given by

$$K_c = \frac{1}{a}\left(\frac{b}{b-c}\right). \tag{47}$$

The infected mice population at infinite time is found to vanish if $K \leq K_c$ but to be nonzero otherwise. Field studies [45] indeed show such behavior including the fact that, if ecological conditions at a place in the landscape get temporarily adverse for the mice (as the result of a drought, for example) the infection can drop to zero. (See, for instance,

[3] Although called the 'carrying capacity' by Abramson and Kenkre in [44], K differs from what is normally denoted by that phrase by a multiplicative factor, e.g., $(b-c)$, and will be therefore simply referred to as the *control parameter* here.

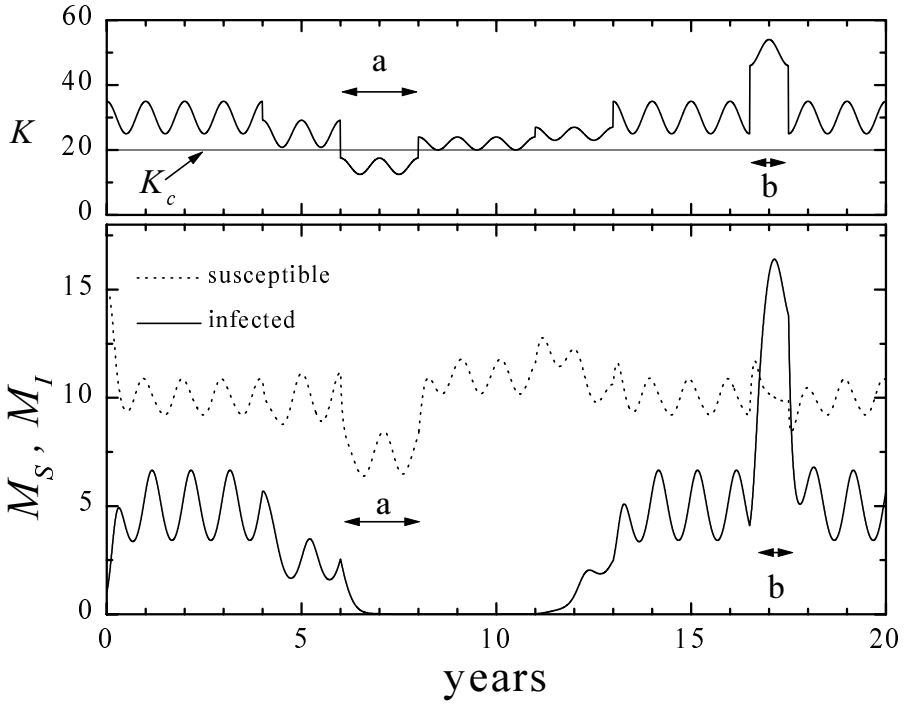

FIGURE 5. Changes in ecological conditions reflected in temporal infection patterns. If the control parameter K falls below the critical value (as in a drought), infection disappears after a lag. If K shows an upward surge, infection follows suit.

Fig. 5). We have recently found simple but exact solutions of (45), (46) in the absence of diffusion, which lead to these bifurcations, described numerically in [44]. We present them below.

Noticing as in [44] that the addition of (45), (46) yields a Fisher equation for the *total* mice density,

$$\frac{\partial M}{\partial t} = (b-c)\,M - \frac{M^2}{K} + D\frac{\partial^2 M}{\partial x^2}, \tag{48}$$

we use the substitution $y = 1/M$ to get a linear equation for y in the absence of D,

$$\frac{dy}{dt} + (b-c)\,y = \frac{1}{K}, \tag{49}$$

which is solved at once. The solution for $M(t)$ is, then, generally,

$$M(t) = \frac{1}{\frac{e^{-(b-c)t}}{M(0)} + \int_0^t dt' \frac{e^{-(b-c)(t-t')}}{K(t')}}. \tag{50}$$

If we rewrite (46) in the absence of D as

$$\frac{dM_I}{dt} - f(t) M_I + aM_I^2 = 0, \tag{51}$$

where $f(t)$ is given in terms of the exact expression (50) as

$$f(t) = -c + M(t)\left(a - \frac{1}{K(t)}\right), \tag{52}$$

we can use the same reciprocal transformation as above to solve (51). The result for the infected population is the exact expression

$$M_I(t) = \frac{1}{\frac{G(t,0)}{M_I(0)} + a\int_0^t dt' G(t,t')}, \tag{53}$$

$$G(t,t') = \exp\left[-\int_{t'}^{t} f(s)\, ds\right]. \tag{54}$$

Explicit solutions for various given time variations of $K(t)$ can be obtained to produce graphs as in [44], or as in Fig. 5, but fully analytically.

If we restrict attention to time-independent K, (50) simplifies to

$$M(t) = \frac{1}{\frac{e^{-(b-c)t}}{M(0)} + \frac{1-e^{-(b-c)t}}{K(b-c)}}. \tag{55}$$

In the trivial case that the birth rate is exceeded by the natural death rate, the total mice population decays to zero. This is uninteresting. In the other case, $b-c$ is positive and $M(t)$ settles from whatever initial value to the saturation value $K(b-c)$. By approximating the total mice density $M(t)$ by this saturation value, we see that (52) gives

$$f(t) \approx f(\infty) = -c + K(b-c)\left(a - \frac{1}{K}\right) = -b + a(b-c)K. \tag{56}$$

Note that $f(\infty)$ vanishes for the critical value of the control parameter K_c given by (47), and can be generally written as

$$f(\infty) = a(b-c)(K - K_c). \tag{57}$$

Clearly, $f(\infty)$ changes sign as K varies from being greater than, to smaller than, K_c. If the former, $G(t,0)$ in (53) decays to zero and the term $\int_0^t dt' G(t,t')$ yields a finite result as t increases without limit. Under the approximation $f(t) \approx f(\infty)$, this finite result is $[a(b-c)(K-K_c)]^{-1}$ so that (53) yields, for the limiting value of the infected mice,

$$M_I(\infty) = (b-c)(K - K_c). \tag{58}$$

If, however, $K < K_c$, the denominator of (53) blows up and

$$M_I(\infty) = 0. \tag{59}$$

This *dynamical* explanation of the bifurcation shows how temporal patterns in the hantavirus infection arise directly from temporal variations in the ecological parameter $K(t)$. An extension of this idea has led to the understanding [44] of the emergence of *spatial patterns* in the hantavirus, observed in the field [46], and known by the term 'refugia'. These refugia, which correspond to reported indications of 'focality of the infection', stem from the mobility of the mice over the terrain and the diversity of the landscape. The former is described by the diffusive terms in (45), (46), and the latter by a spatial dependence in the control parameter $K(x)$. Generally, a 3-dimensional dependence may be used, but practically, a 2-dimensional description suffices. Application of these ideas to fully realistic landscapes may be found in [47]. Because the Fisher equation is not analytically soluble, we have recently studied some of its modifications. Exact solutions of two of these modified equations also show analytically the occurrence of refugia [48].

We refer the reader to the literature where a good deal of further development of these ideas has been carried out from the AK model including the examination of fluctuations [49] and the validity of moment equations, and the study of waves of infection [50] emanating from the refugia. The study of fluctuations is based on simulations, and addresses the obvious shortcoming of the AK model that it deals with continuous mouse densities, and results [49] in consequences such as a shift in K_c, the critical value of the control parameter responsible for the bifurcation onset (see Fig. 6.) Waves of the hantavirus [50] are fascinating consequences of our analysis, have special importance in these troubled days in the context of bioterrorism, and have been excellently described by Abramson elsewhere in these Proceedings.

Bacteria in Petri Dishes

Exceedingly pretty patterns [51] characterize the evolution of bacterial colonies. A subject of obvious medical importance, such evolution has been studied recently [51–57] experimentally as well as theoretically. The Fisher equation that we have encountered in this article in the hanta context as applying to the sum of the infected and susceptible mice, but not to each class individually, resurfaces here directly in the description of the bacterial population. In terms of the respective parameters a (growth rate), b (competition parameter), and D (diffusion coefficient), the basic equation governing the spatio-temporal dynamics of the bacterial population $u(x,t)$ is taken to be

$$\frac{\partial u(x,t)}{\partial t} = D\frac{\partial^2 u(x,t)}{\partial x^2} + au(x,t) - bu^2(x,t). \tag{60}$$

A lucid set of lectures on this topic were delivered by Lin in the PASI but are unfortunately not part of her Proceedings article which focuses on other interesting areas of pattern formation. We describe below theoretical studies that were stimulated by those lectures.

First we point out that the logistic part of the Fisher equation (i.e., (60) without the diffusion term), has a simple physical origin in the bacterial context. Start with two coupled equations for the bacterial density $u(x,t)$ and a food density $f(x,t)$ such that

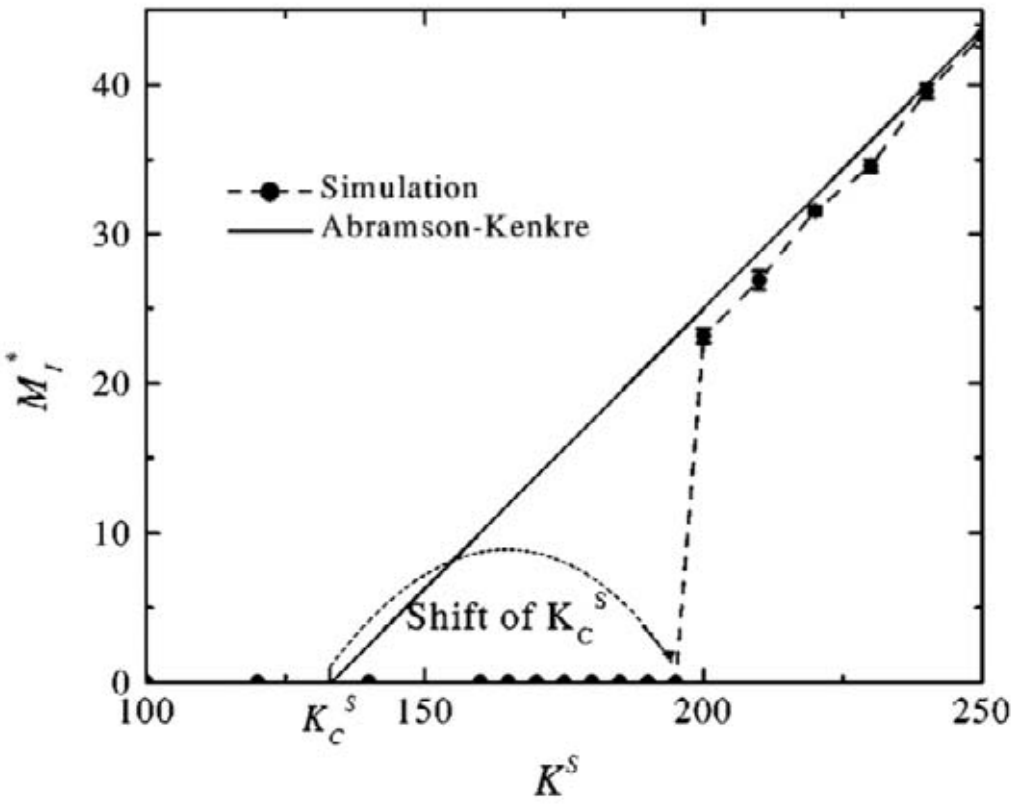

FIGURE 6. Shift of the critical value of the control parameter relative to the prediction of the AK model resulting from simulation analysis which incorporates the effect of finiteness of the population and the discreteness of the mice number. Parameter values are arbitrary.

the rate of change of each of the densities is proportional to their product uf. The proportionality constants, respectively A and $-B$, are different in value and opposite in sign since the food is eaten by the bacteria. Cross-multiplying the proportionality constants and adding, we find that $Bu+Af$ is an invariant and therefore equal to its own initial value. Solving for f and substituting in the u equation leads, effortlessly, to the logistic evolution for u. A clear meaning may also be assigned in this fashion to the a and the b of the Fisher equation in terms of the initial values of the food and the bacterial densities.

Returning to the experiments that have been carried out on bacterial evolution in Petri dishes, we observe that such experiments have employed moving masks [55] and have resulted in reports of extinction transitions suggested earlier in theoretical calculations [56] as well as in numerical simulations [57]. The focus of the theoretical calculations has been on systems in which the growth rate a varies from location to location in a *disordered* manner, and in which linearization of the Fisher equation (60) makes sense. Such linearization has made possible the use of concepts from Anderson localization [59], a phenomenon well-known in the solid state physics of quantum mechanical

systems. It is likely, however, that the nonlinear features represented by $-bu^2$ in the Fisher equation are important and may not be relegated to a secondary role. It is possible, as we show next, to carry out interesting analysis of the system while retaining the full nonlinearity of the competition term.

As in the moving mask experiments [55], we consider an effectively linear Petri dish in which a mask shades bacteria from harmful ultraviolet light. The light causes the bacteria to die in regions outside the mask. They grow in regions under the mask. Contrary to the situation in previous analyses, however, we do not allow the mask to move. Focusing attention on *stationary* masks, we analyze the x-dependence of the stationary population of the bacteria. As in previous considerations [55], we assume that the growth rate has a positive constant value a inside the mask, and a negative value outside the mask. It is perhaps interesting to note here that inhomogeneity in resources appears to be customarily represented in the K term in the hantavirus context, which would correspond to the b term here, but that it is taken into account via the a term in the bacterial context. Arguments could be given in support of such a distinction but the choice is largely arbitrary. Realistically, both a and b here should be affected by resource differences.

First, let us take the value of a outside the mask to be negative infinite to reflect extremely harsh conditions (due to ultraviolet light) when the bacteria are not shaded from the light. This makes the population at the mask edges, and outside, to be identically zero. The boundary conditions are thus of the Dirichlet form. In the steady state, introducing $\xi = x/\sqrt{D}$ for simplicity, we obtain the ordinary differential equation for the stationary population $u(\xi)$:

$$\frac{d^2u(\xi)}{d\xi^2} + au(\xi) - bu^2(\xi) = 0. \tag{61}$$

Our interest is in the regions in the interior of the mask of width $2w$, i.e., for $-w \leq x \leq w$, the boundary conditions being $u\left(\pm w/\sqrt{D}\right) = 0$. How can we give a practical prescription to decide on the applicability of the Fisher equation to bacterial evolution with this setup? And how can we extract the parameters D, a, b from observations if the equation is found to be applicable? These are the questions we now address.

The answers are straightforward [60]. Solutions of (61) can be written in terms of the Jacobian elliptic function $cd = cn/dn$:

$$u_i(\xi) = (a/b)\left[\, f_\alpha(k)\,\mathrm{cd}^2\left(\sqrt{a}\,f_\beta(k)\,\xi, k\right) + f_\gamma(k)\right]. \tag{62}$$

The solution involves the Fisher parameters a, b and three functions of k alone:

$$\begin{aligned} f_\alpha(k) &= (3/2)\,k^2\left(k'^2 + k^4\right)^{-1/2} \\ f_\beta(k) &= (1/2)\left(k'^2 + k^4\right)^{-1/4} \\ f_\gamma(k) &= (1/2)\left[1 - \left(k^2+1\right)\left(k'^2 + k^4\right)^{-1/2}\right], \end{aligned} \tag{63}$$

with $k'^2 = 1 - k^2$. Fitting (62) to the observed stationary profile would yield a, b, k. For sensitivity purposes the nome $q = \exp(-\pi K'/K)$, rather than k, should be used for

fitting [60]. Once k is found, the determination of the diffusion constant D follows in the light of the Dirichlet boundary condition that u_i vanishes at $\xi = \pm w/\sqrt{D}$.

An interesting effect involving a critical mask size emerges from the analysis [60]. For any size, there is a conflict between the growth process which tends to bring the bacterial population to its saturation value, and the diffusion process which tends to move the population out of the mask where it dies because of the adverse conditions. This conflict is won by the diffusion process if the mask size is below a certain critical value; a steady-state population then cannot be supported. There is, therefore, an abrupt transition at a critical value of the size. This result is similar to one known in the study of phytoplankton blooms [61]. We have recently suggested [60] that it be used observationally to validate the Fisher equation in bacterial populations. Indeed, for a given set of Fisher parameters, a decrease in the mask width $2w$ from large values causes a monotonic decrease in k. The value $k = 0$ is reached at a finite value of the width. This vanishing of k means that the elliptic function $\mathrm{cd}(\beta\xi, k)$ becomes its trigonometric counterpart $\cos(\beta\xi)$, and one gets $\cos^2\left(\frac{w}{2}\sqrt{a/D}\right) = 0.5$, showing that a critical size $2w_c$ of the mask exists:

$$2w_c = \pi\sqrt{\frac{D}{a}}. \tag{64}$$

It is relatively easy to estimate a value of a from suitable monitoring of bacterial growth [55] but much more difficult to arrive at a reasonably precise value of D. On the basis of quoted [55, 57] values, $D \approx 10^{-5}$ cm^2/s, $a \approx 10^{-4}$/s, the critical mask size can be calculated [60] to be of the order of half a cm. Since masks of this size are easy to use, there is hope that the effect might be observable in the bacterial context. Dirichlet boundary conditions used in the previous analysis are not appropriate if we relax the condition that the environment outside the mask is harsh enough to ensure zero population of the bacteria. In such a case, the critical size becomes smaller than that in the Dirichlet case [60, 61]. Line (b) in Fig. 7 shows for this case the dependence of the maximum of the bacterial density in the mask while line (a) shows the case with Dirichlet boundary conditions. In the inset are shown the stationary profiles for several mask sizes for the non-Dirichlet case. The tendency towards extinction as the mask size approaches the critical value is clear [60].

Much further exploration of Fisher-like equations has been carried out recently for bacterial evolution. It includes solutions of a nonlinear drift equation applicable to bacteria whose diffusion constant is practically negligible [62], and pattern formation from the Fisher equation in the presence of long-range, i.e., spatially nonlocal, competition interactions [63]. We comment briefly on each.

If the bacteria move via a convection term $v\partial u(x)/\partial x$, where v is an externally imposed velocity, instead of diffusively as in the Fisher equation, analytic solutions can be written down for a number of physically relevant situations. As one example, we give

$$u(x,t) = \frac{1}{\frac{e^{-at}}{u_0[x-(v_0/\omega)\sin\omega t]} + \frac{b}{a}\left(1-e^{-at}\right)}, \tag{65}$$

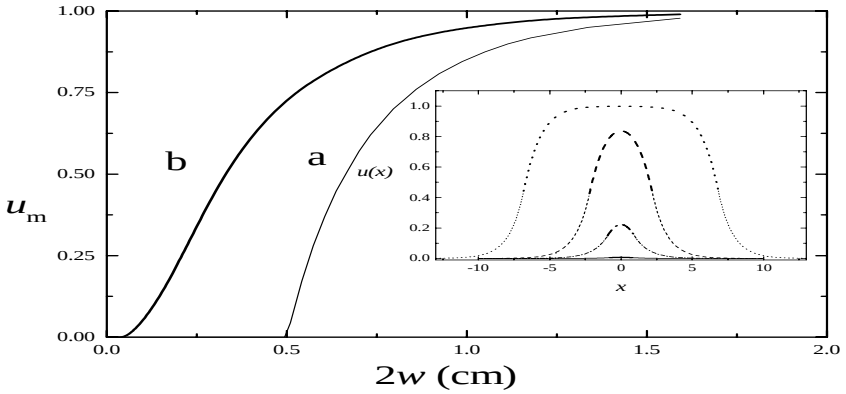

FIGURE 7. Critical effect of mask size showing that bacteria cannot be supported below a critical size because they diffuse out of the mask into the hostile environment.

which describes the exact evolution of the bacterial density when the velocity varies sinusoidally in time as $v_0 cos\omega t$ but a and b are constant. As another example, we show

$$u(x,t) = \frac{1}{\frac{e^{-\frac{1}{v}\int_{x-vt}^{x} dx' a(x')}}{u_0[x-vt]} + b\int_0^t dt' e^{-\frac{1}{v}\int_{x-vt'}^{x} dx' a(x')}}, \tag{66}$$

which applies when v and b are constant, but $a(x)$ is space-dependent as when there is a mask [62].

What happens if we return to the Fisher equation (with its diffusive term) but modify it to include a nonlocal competition term? Such a term would describe bacteria competing with other bacteria not only at their own location but also at finite distances. Nonlocal competition of this kind could come about from a variety of sources such as fast motion of nutrients. Let the competition occur via an 'influence function' $f_\sigma(x-y)$ whose range is σ. Thus, let

$$\frac{\partial u(x,t)}{\partial t} = au(x,t) + D\frac{\partial^2 u(x,t)}{\partial x^2} - bu(x,t)\int f_\sigma(x-y)\,u(y,t)\,dy. \tag{67}$$

The Fisher equation is one extreme limit of (67) when $f_\sigma(x-y) = \delta(x-y)$. The other extreme, in which the influence range is infinite, is trivial to solve analytically. Integration of (67) over x shows that the quantity $\overline{u}(t) = \int u(x,t)\,dx$ obeys the logistic equation. Its solution is obtained as in (50) or (55):

$$\overline{u}(t) = \left[\frac{e^{-at}}{\overline{u}(0)} + \frac{b}{a}\left(1-e^{-at}\right)\right]^{-1} = e^{\int_0^t [a-b\overline{u}(s)]ds}\overline{u}(0). \tag{68}$$

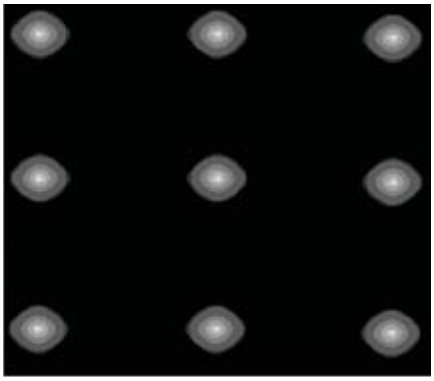

FIGURE 8. Steady-state solution for $u(x,y)$ in a 2-d set up of 30 x 30 sites with periodic boundary conditions with Eq. (67) governing the evolution. Patterns appear as the result of the non-local competition interaction. Lighter regions represent larger values of u. Parameters are arbitrary: $a = b = 1$ and $D = 10^{-2}$ in appropriate units, and the influence function is Gaussian with a range σ of 10 sites.

This means that we have simply the diffusion equation

$$\frac{\partial w(x,t)}{\partial t} = D\frac{\partial^2 w(x,t)}{\partial x^2} \tag{69}$$

for the normalized transformed quantity

$$w(x,t) = \frac{u(x,t)}{[\overline{u}(t)/\overline{u}(0)]}, \tag{70}$$

and that the complete explicit solution for $u(x,t)$ is

$$u(x,t) = \left[e^{-at} + \frac{b\overline{u}(0)}{a}\left(1-e^{-at}\right)\right]^{-1} \int \Psi(x-y,t)\, u(y,0)\, dy, \tag{71}$$

where $\Psi(z,t)$ is the standard Gaussian propagator $(4\pi Dt)^{-1/2} exp(-z^2/4Dt)$ of the diffusion equation. On discrete infinite space, the propagator is made of products of modified Bessel functions and exponentials.

Although exact analytic solutions are possible to obtain in this extreme (because the diffusion and the logistic growth are completely uncoupled), little of striking interest emerges in this extreme. As soon as the range of the influence function is taken to be *intermediate*, noteworthy patterns appear (see, e.g., Fig. 8). Such patterns are not present as predictions of the original Fisher equation. The long-range nonlinear interaction is responsible for their emergence. The nature of the influence function f_σ determines major properties of the patterns, the presence or absence of tails in f_σ being an important factor [63].

NONLINEAR EQUATIONS AND MEMORIES IN COMBINATION

While nonlinear techniques and the memory formalism have little in common, there are systems and phenomena whose study involves the two in combination. We discuss these in three parts: nonlinear equations *with* memories, nonlinear equations which *yield* memories, and nonlinear equations which compete *against* memories.

Nonlinear Equations with Memories

We have seen that the transport of the Fisher equation is incoherent, i.e., governed by diffusion. What are the consequences of replacing it by one with arbitrary degree of coherence? The answer to this question leads to interesting conclusions and may be pursued in several different ways other than by adding drift terms as in the bacteria problem described in the previous section. One of them consists of replacing the diffusion part in the Fisher equation by a wave counterpart [64]; another of replacing it by a combined wave and diffusive form (9) characteristic of the telegrapher's equation [65]; and yet another of replacing it by diffusion but with a memory function attached [66]. We examine each in turn.

If the transport in the Fisher equation is completely coherent, we have

$$\frac{\partial^2 u(x,t)}{\partial t^2} = v^2 \frac{\partial^2 u(x,t)}{\partial x^2} + au(x,t) - bu^2(x,t). \tag{72}$$

Traveling wave solutions of the kind $u(x-ct) = U(z)$, where z is $x-ct$, satisfy

$$\frac{d^2 U(z)}{dz^2} + \frac{aU(z) - bU^2(z)}{v^2 - c^2} = 0, \tag{73}$$

which can be solved exactly. We may cite, as an example, the solution

$$u(x,t) = \frac{3}{2}\left\{ sech^2 \left[\left(\frac{x-ct}{2} \right) \sqrt{\frac{k}{c^2 - v^2}} \right] \right\}, \tag{74}$$

which applies to the scaled case when the expression $au - bu^2$ is written as $ku(1-u)$. If the variance of the solution is called σ, the speed c of this profile is found [64] to obey

$$c^2 = v^2 + k\left(\sqrt{2}\pi^2\sigma^2\right)^{2/3}. \tag{75}$$

The striking conclusion that emerges from the analysis of other similar coherent equations is that, in contrast to the Fisher equation, the coherent transport case supports two kinds of *coexisting* solutions: anti-fronts as well as fronts [64].

If the transport in the Fisher equation is only partly coherent, the Fisher equation may be replaced by

$$\frac{\partial^2 u(x,t)}{\partial t^2} + \alpha \frac{\partial u(x,t)}{\partial t} = v^2 \frac{\partial^2 u(x,t)}{\partial x^2} + au(x,t) - bu^2(x,t) \tag{76}$$

as in [65]. The transport part is a telegrapher's equation, equivalently, a diffusion equation with an exponential memory appended. Two kinds of new results relative to the Fisher equation appear: generalization of Fisher results to include finite correlation times of transport, and unexpected results not known earlier. To the latter kind belongs the existence of a speed beyond which *spatial* oscillations appear in the wave-front shape, and the possibility of wave trains of infinite extent [65].

While (76) is certainly an allowable manner of introducing partial transport coherence into the Fisher equation, there is an obvious alternative. Instead of first generalizing the transport part of the Fisher equation by incorporating an exponential memory, converting the resulting integro-differential equation via differentiation into a differential equation, and finally adding the nonlinear logistic term to obtain the starting point of the analysis, we may take as our point of departure,

$$\frac{\partial u(x,t)}{\partial t} = D\int_0^t \phi(t-\tau)\frac{\partial^2 u(x,t)}{\partial x^2}d\tau + f(u), \tag{77}$$

where $f(u) = au(x,t) - bu^2(x,t)$. This equation reduces to the Fisher equation if the memory function $\phi(t)$ is a $\delta-$function in time. If $\phi(t) = \alpha e^{-\alpha t}$, we obtain

$$\frac{\partial^2 u}{\partial t^2} + [\alpha - f'(u)]\frac{\partial u}{\partial t} = v^2\frac{\partial^2 u}{\partial x^2} + \alpha f(u), \tag{78}$$

where $D\alpha = v^2$. In contrast to (76), the starting point (78) is characterized by a nonlinear damping term. The investigation [66] of this equation reveals an expression for the minimum speed of wavefronts

$$c \geq c_{min} = v\frac{1}{\sqrt{1+\frac{1}{4}(y-1/y)^2}}, \tag{79}$$

where $y = \sqrt{\alpha/k}$. Again we use here, for simplicity, the scaled form with a single k instead of a and b. This minimum speed expression is different from that obtained [65] from (76) and different also from the result of the Fisher equation: $c_{min} = 2\sqrt{kD}$ (see for example [67]). If we make the formal identification $D\alpha = v^2$, as in (9), the Fisher result becomes

$$c \geq c^F_{min} = 2v\sqrt{1/y^2}, \tag{80}$$

whereas the telegrapher's result as obtained in [65] is

$$c \geq c^{MHK}_{min} = v\frac{1}{\sqrt{1+\frac{1}{4}y^2}}. \tag{81}$$

Reaction-diffusion systems in which the transport process is wave-like at short times and diffusive at long times provide, thus, an arena for the combination of memory functions and nonlinear techniques. The passage of the character of the motion from coherent to incoherent is a general feature of all physical systems. So is nonlinearity. We

have noticed that our generalizations converge to the Fisher equation result in the limit of diffusive transport but sharp differences occur in the wave-limit. These include new kinds of solutions we have not mentioned here for lack of space, which involve "inverse" fronts, in which the state $U = 0$ invades the state $U = 1$ [66]. For these and other aspects we refer the reader to the literature.

Nonlinear Equations which yield Memories

Projection operators explained earlier in this article for derivation of memory functions have been clearly fashioned to be used in the context of linear equations. Could they have any utility in conjunction with *nonlinear* equations? Our obvious intuitive answer would be that they would not. We now give a remarkable instance [68] in which they *are* useful, perhaps contrary to expectation.

The result we will obtain is that, starting from the discrete nonlinear Schrödinger equation (40), explicit and exact prescriptions can be written for a GME with nonlinear memories, and that, in particular, the probability difference p of the two sites in a dimer as in (24), obeys

$$\frac{dp(t)}{dt} + 4V^2 \int_0^t ds\; p(s) \cos\left[\chi \int_s^t dz\; p(z)\right] = 0 \tag{82}$$

which displays a memory function *nonlinear* in the probability difference

$$\mathscr{W}(t,s) = 2V^2 \cos\left[\chi \int_s^t dz\; p(z)\right]. \tag{83}$$

We begin with the DNLSE (40) expressed as a density matrix equation

$$\frac{d\rho_{mn}}{dt} = -i\left[V,\rho\right]_{mn} + i\left(L_\chi \rho\right)_{mn}, \tag{84}$$

and note that we could define the nonlinear operator L_χ in one of two ways. For any operator O, we could either choose the definition

$$\left(L_\chi O\right)_{mn} = \chi\left(O_{mm} - O_{nn}\right) O_{mn}, \tag{85}$$

or the definition

$$\left(L_\chi O\right)_{mn} = \chi\left(\rho_{mm} - \rho_{nn}\right) O_{mn}. \tag{86}$$

Use of the first of these in conjunction with a diagonalizing projection operator $\mathscr{P}$ does indeed agree with our 'intuition' that projection operators should be of no value in conjunction with nonlinear equations. The other definition, however, makes the second of the Zwanzig equations (13) formally linear! That linearity is all that is required to make the procedure go through without problems, and to result in a usable GME. The memory functions obtained are generally complicated. A simple form, approximate for extended systems, but exact for a two-site (dimer) system, is

$$\mathscr{W}_{mn}(t,s) = 2V^2 \cos\left[\int_s^t dz\; \left(E_m(z) - E_n(z)\right)\right]. \tag{87}$$

The site energies E are proportional to the probabilities of occupation of the sites because of the nonlinearity inherent in the original equation (40). Thus, we have (82).

The meaning of the nonlinear GME (82) is surprising. The definition of a new quantity ξ through

$$\xi(t) = \int_0^t ds\, p(s) \tag{88}$$

allows us to rewrite (82) in the form of the differential equation

$$\frac{d^2\xi(t)}{dt^2} + \frac{4V^2}{\chi}\sin[\chi\xi(t)] = 0, \tag{89}$$

which is nothing other than the familiar equation obeyed by the displacement of the classical physical pendulum under the action of gravity. It can be solved at once in terms of elliptic functions and shown to yield results completely equivalent to the selftrapping results of (43).

Nonlinear Equations which compete against Memories

Evolution equations at the macroscopic level of description take forms which are substantially different from evolution equations at the microscopic level. Generally accepted lore assumes the latter to be linear, local, and reversible. The former are found to be sometimes nonlinear, sometimes nonlocal in time and space, and often irreversible. The problem of the passage from microscopics to macroscopics has always been a central concern of statistical mechanics. Whether one or the other form of macroscopic equations is appropriate and compatible with the given microscopic starting point (typically Newton's or Schrödinger's equation) is obviously an important question. In certain contexts this question takes the form of a competition between a nonlinear equation and a linear equation, the latter sometimes with memory. An example is found in condensed matter physics systems in which electrons or other moving quasiparticles interact strongly with vibrations, with the resulting phenomenon of polaronic selftrapping and the emergence of entities such as Davydov solitons [38]. Intellectual wars have been waged on this subject. Early objections to the nonlinear equation raised on general grounds [30], more recent arguments based on Wigner distribution functions [31], and even more recent studies based on explicit numerical solutions of simple models [32] have combined to show that polaronic systems are not well served by a description based on the discrete nonlinear Schrödinger equation. It has been additionally found that a memory function analysis [8] does a much better job for many parameter ranges of interest. For want of space we give no discussion here but only direct the reader to the vast literature on the subject (see, e.g., [31], [33], and references therein).

In concluding this section on nonlinear techniques, we emphasize the emergence of *thresholds* in nonlinear systems. Excitons or electrons obeying the DNLSE (40) are free to move or become selftrapped in localized regions as the critical parameter χ/V passes a threshold value. Infection appears or disappears in mice as the control parameter K, determined by resources such as vegetation, exceeds a certain magnitude. Bacterial populations vanish or survive under masks shading them from lethal ultraviolet

light according to whether the mask size is smaller or larger than a threshold. Spatial oscillations in shock fronts make their abrupt appearance as steepness or speed crosses a critical value. Such interesting occurrences are quite out of bounds to linear equations and to linear methods of surveying the world.

MISCELLANEOUS TECHNIQUES BASED ON KINETIC EQUATIONS

The diversity of phenomena encountered in the practice of statistical mechanics surely requires that one go beyond the memory formalism or the nonlinear techniques described thus far in this article. In this final section of the article we illustrate two approaches lying outside the memory/nonlinear regimes. One of them uses the Fokker-Planck equation, the other the (linear) Boltzmann equation.

Fokker-Planck Techniques

The quantum world underlying all phenomena around us is generally very different from the classical world visible at the macroscopic level. Nevertheless, there are mathematical similarities in the methods of analysis. We begin by treating two problems, one concerning the classical phenomenon of microwave heating in ceramic materials, the other concerning the quantum motion of charge carriers in an organic crystal. The tool we will use for the study of both is the Fokker-Planck equation. The mathematics we will employ for the solution of that equation will be identical. The results will turn out to appear, however, completely different. In the study of microwave heating of ceramic materials [70], one is interested in analyzing the absorption of electromagnetic radiation by moving ions or vacancies in a solid. Therefore, one studies the motion of a charge in a spatially periodic potential under the simultaneous action of an external field and of random forces responsible for thermalization. Under the high-damping approximation, the governing equation for the probability density function $P(x,t)$ is of the Fokker-Planck (or Smoluchowski) form [69]

$$\frac{\partial P(x,t)}{\partial t} = \frac{1}{m\alpha}\frac{\partial}{\partial x}\left[\left(\frac{dU}{dx} - qE\right)P(x,t) + \frac{1}{\beta}\frac{\partial P(x,t)}{\partial x}\right]. \tag{90}$$

Here m and q are the ionic mass and charge respectively, E is the electric field of the microwave, α is representative of bath interactions, and β is proportional to the reciprocal of the temperature as defined earlier.

In investigations of the mobility of photoinjected charge carriers in strong electric fields, one begins with the effective mass equation for a carrier augmented by Brownian motion terms. The resulting Langevin equation leads, via standard methods such as those explained by Wio and Lindenberg elsewhere in these Proceedings, to the Fokker-Planck equation [72] for the distribution function $f(k,t)$ in k-space

$$\frac{\partial f(k,t)}{\partial t} = \frac{1}{\hbar^2}\frac{\partial}{\partial k}\left[\left(\gamma\frac{d\varepsilon_k}{dk} - \hbar qE\right)f(k,t) + \frac{1}{\beta}\frac{\partial f(k,t)}{\partial k}\right], \tag{91}$$

where γ is a friction coefficient.

There is a clear analogy between the position variable x and the crystal momentum k, and between the potential $U(x)$ and the band energy ε_k. The latter two are both periodic and often well represented by sinusoids. In both cases, the observable of interest is the average steady-state drift velocity as a function of the field E. The computational procedure is to put the time derivative of the distribution function equal to zero, and to solve the resulting first-order differential equation for the derivative of the distribution function. The details may be found in [69] or [72].

Given that the two problems appear to be essential identical, it is remarkable that the field dependence of the velocity is sharply different in the two cases. Fig. (9) makes this difference clear. The (normalized) drift velocity in each case is plotted against the (normalized) electric field for different values of the (normalized) temperature, v_0 and v_{max}, E_0 and E_c, and $2U_0$ and V, being the respective normalization quantities.[4] The carrier velocity shows activated behavior in the classical system of microwave heating. The temperature increases upwards in the curves in the upper frame. At low temperatures, the average drift velocity is negligible and picks up only at temperatures high enough to kick the ion (carrier) out of the potential well which confines it. Once the temperature is high enough, sufficiently large fields tilt the periodic potential so sharply that the corrugation characteristic of the atomic potential makes negligible contribution. The velocity is then linear in the field, increasing with field as it would for a free particle. This behavior, visible in the upper frame of Fig. (9), should be contrasted with what one encounters in the lower frame which depicts the hole or electron in the organic crystal. The low-field behavior is Ohmic: the carrier velocity is proportional to the field. At higher fields, the velocity *decreases* as the field increases. This negative differential mobility phenomenon occurs at all temperatures. Note that, contrary to the upper frame in Fig. (9), the lower frame has temperature increasing downwards among the curves. At low temperatures, the transition from the Ohmic increase to the further decrease is sharper, the transition at zero temperature displaying a prominent cusp. Physically, the transition signals Bloch oscillations: the carrier exits the Brillouin zone at one end and reenters it at the opposite end. Being proportional to the derivative of the band energy, the velocity varies non-monotonically in the zone as a function of k. As the carrier samples regions in the zone where the velocity is smaller, the average drift velocity decreases. This is what yields negative differential mobility.

We have thus seen that it is not difficult to gain a physical understanding of the sharp difference between the classical and quantum problems we have considered. But how is this difference reflected in the calculations? The answer lies in the manner the drift velocity is computed from the distribution function. In the organic crystal case, once $f(k) = f(k,\infty)$ is found, one calculates the average of the velocity through the prescription $\langle v\rangle = (1/\hbar)\int (d\varepsilon_k/dk) f(k)\, dk$: the carrier velocity in a band is related straightforwardly to the band energy. In the classical microwave heating case, the ion velocity is not given by the average of the $x-$derivative of the potential $U(x)$ in the same way but is obtained quite differently. The high-damping (Aristotelian) approximation used in the treatment of this problem means that the velocity is proportional to the force. This force

[4] It is not important in the present context to specify their detailed meaning, for which see [72].

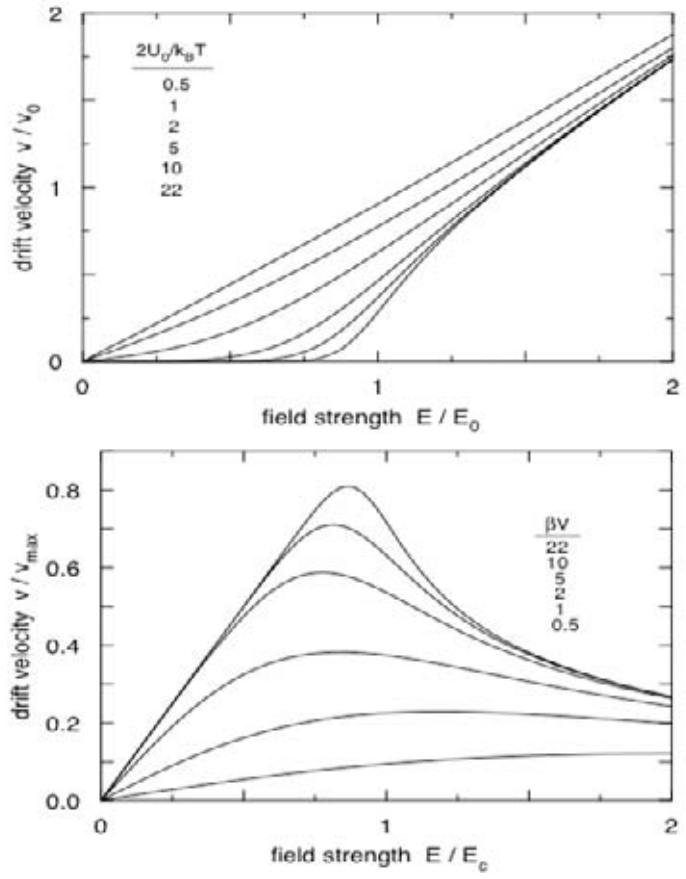

FIGURE 9. Strikingly different nonlinear dependences of carrier velocity on electric field obtained essentially from the same mathematical content of the Fokker-Planck equation in two cases: (upper graph) classical motion in regard to microwave heating in a ceramic material, and (lower graph) quantum motion of a charge carrier in an organic crystal.

is the sum of the electric force qE and the potential force $-dU(x)/dx$. The noteworthy difference in the classical expression for the velocity is that, relative to its quantum counterpart, there is a change of sign as well as an additive component (proportional to the field). This difference is responsible for the curious apparent discrepancy in the velocity behavior in the two parts of Fig. (9). If the lower frame curves in Fig. (9) are reflected about the field axis to represent the change in sign, and a term linear in the

field is then added to it, one indeed obtains the curves in the upper frame in Fig. (9) in the correctly reversed temperature order. In fact, the expressions for the average drift velocity derived for the microwave heating problem of (90) and for the charge carrier problem of (91) respectively, show this relationship clearly. The drift velocity is given in the former (classical) situation by

$$\langle v\rangle = \frac{2}{\beta m\alpha\ell}\frac{\sinh(\beta qE\ell/2m\alpha)}{I_{-i\beta qE\ell/2\pi m\alpha}(2\beta U_0)I_{i\beta qE\ell/2\pi m\alpha}(2\beta U_0)}, \tag{92}$$

and in the latter (quantum) situation by

$$\langle v\rangle = \frac{qE}{\gamma} - \frac{1}{\pi}\frac{a\sinh(\pi\bar{h}\beta qE/\gamma a)}{\beta\bar{h}I_{-i\bar{h}\beta qE/\gamma a}(2\beta V)I_{i\bar{h}\beta qE/\gamma a}(2\beta V)}, \tag{93}$$

where $I_\nu(z)$ is the modified Bessel function of (imaginary) order ν and argument z, and U_0, V are proportional to the peak values of the respective potentials ($U(x)$ and the band energy). The quantity ℓ in (92) is the spatial period of the potential and is analogous to $2\pi/a$ in (93). It is amusing that the same mathematics leads to completely different behaviors for the drift velocity.

The investigation of the quantum carrier velocity dependence on the electric field explained above was recently undertaken [73] to verify an idea related to velocity saturation observed in the organic crystal naphthalene [71] and later claimed also to be observed in pentacene. The idea being verified was that such saturation is a consequence of the nonparabolic nature of bands in organic crystals. As we have seen above, velocity saturation at high fields cannot arise merely from the band being sinusoidal (nonparabolic), the natural consequence of such nonparabolic bands being negative differential mobility. This means a *decrease* in the velocity at high fields, not a saturation. In the next section we will reexamine this issue of saturation from a starting point different from the Fokker-Planck equation.

Other Kinetic Equation Techniques

One of the quantum kinetic equations widely used to describe transport is the so-called Stochastic Liouville equation (SLE) for the density matrix ρ of the carrier, employed extensively in exciton transport in molecular crystals [6]. In terms of the representation of Wannier states m, n, etc., it is written as

$$\begin{aligned} i\bar{h}\frac{d\rho_{m,n}}{dt} &= [V,\rho]_{m,n} + (qEa)(m-n)\rho_{m,n} \\ &\quad -i\bar{h}\alpha_0(1-\delta_{m,n})\left[\rho_{m,n}-\rho^e_{m,n}\right] \end{aligned} \tag{94}$$

where the scattering is represented by the single relaxation rate α_0 at which the off-diagonal elements of the density matrix relax to their equilibrium values $\rho^e_{m,n}$ in the absence of the field. By Fourier-transforming the SLE to k-space, the distribution function

$$f(k) = \langle k|\rho|k\rangle = \frac{a}{2\pi}\sum_{m,n}\rho_{m,n}e^{ika(m-n)}, \tag{95}$$

obtained from the diagonal part of ρ in reciprocal space, is found to obey

$$\frac{\partial f(k,t)}{\partial t} = -\mathscr{E}\frac{\partial f(k,t)}{\partial k} - \alpha_0\left[f(k,t) - f^{th}(k)\right], \tag{96}$$

where $\mathscr{E} = qE/\hbar$ and $f^{th}(k)$ is the thermal distribution. Equation (96) is restricted in its applicability to high temperatures because it contains a *single* relaxation time $1/\alpha_0$. A more accurate description is provided by its counterpart with arbitrarily $k-$dependent relaxation times $1/\alpha_k$:

$$\frac{\partial f(k,t)}{\partial t} = -\mathscr{E}\frac{\partial f(k,t)}{\partial k} - \alpha(k)\left[f(k,t) - f^{th}(k)\right]. \tag{97}$$

In the condensed matter physics community [75], this equation is called the linear Boltzmann equation under the relaxation time approximation[5]. It, or its more general form which displays the transition rates from one $k-$state to another [75], is not bilinear in the distribution function as in the case introduced by its originator, Boltzmann. The bilinear form, explained elsewhere in these Proceedings by Romero-Rochín, is appropriate for the kinetic theory of gases in which molecules collide against molecules. The present *linear* form is appropriate in electron and hole transport theory in which transitions are assumed to occur because of interactions of the carriers with other objects such as impurities and phonons rather than with themselves.

The Boltzmann equation is traditionally used in textbook treatments of the mobility of carriers under the approximation that the electric field is weak enough that only linear terms in the field need be retained. By contrast, we will give here an analysis [73] which is valid for arbitrarily strong field strengths and for arbitrary k-dependence of $\alpha(k)$.

Rewriting (97) in terms of the linear operator $\alpha + \mathscr{E}\,\partial/\partial k$, and constructing the Green function $G(k,t) = \exp\left[-t\left(\alpha + \mathscr{E}\frac{\partial}{\partial k}\right)\right]$, the solution is written down at once:

$$f(k,t) = G(k,t)\,f(k,0) + \int_0^t ds\, G(k,s)\,\alpha(k)\,f^{th}(k). \tag{98}$$

The identity

$$e^{c(A+B)} = e^{cA}e^{\int_0^c dx\, e^{-xA}\,B\,e^{xA}} \tag{99}$$

where c (or x) is a $c-$number and A and B are generally non-commuting operators not involving time, is easily proved. Applied to (99), it gives

$$e^{-t\left(\alpha+\mathscr{E}\frac{\partial}{\partial k}\right)} = e^{-\mathscr{E}t\frac{\partial}{\partial k}}e^{-\int_0^1 dx\, e^{x\mathscr{E}t\frac{\partial}{\partial k}}\,\alpha t\, e^{-x\mathscr{E}t\frac{\partial}{\partial k}}}. \tag{100}$$

---

[5] This form, ubiquitous in solid state treatments, has served as the basis of an enormous number of practical computations in realistic applications. An often forgotten peculiarity it possesses is that it cannot conserve probability at all times. This is clear on putting the field equal to zero and summing over all k. This feature, which has not stopped generations of solid state investigators (including the present author) from using the form in the region of long times where it is valid, is not possessed by the single-relaxation-time approximation!

Expansion of the integrand and the recognition that $\left[\frac{\partial}{\partial k},\alpha\right]=\partial\alpha/\partial k$ leads to the result that, for any function $\Omega(k)$,

$$e^{-\int_0^1 dx\, e^{x\mathscr{E}t\frac{\partial}{\partial k}}\,\alpha t\, e^{-x\mathscr{E}t\frac{\partial}{\partial k}}}\Omega(k)=e^{-t\int_0^1 dx\,\alpha(k+x\mathscr{E}t)}\Omega(k). \tag{101}$$

Explicit evaluation of the Green function operation is now possible:

$$G(k,t)\,\Omega(k)=e^{-\overline{\alpha}(k-\mathscr{E}t,t)t}\Omega(k-\mathscr{E}t) \tag{102}$$

for any function $\Omega(k)$. Here

$$\overline{\alpha}(k,t)=\frac{1}{\varepsilon t}\int_k^{k+\mathscr{E}t}\alpha(y)\,dy \tag{103}$$

is the average of the reciprocal relaxation time $\alpha(k)$ over a region in k-space of extent $\mathscr{E}t$ centered around $k+\mathscr{E}t/2$. The general solution of the Boltzmann equation (97) is thus obtained as

$$f(k,t)=e^{-\overline{\alpha}(k-\mathscr{E}t,t)t}f(k-\mathscr{E}t,0)+\int_0^t ds\, e^{-\overline{\alpha}(k-\mathscr{E}s,s)s}\alpha(k-\mathscr{E}s)\,f^{th}(k-\mathscr{E}s). \tag{104}$$

It leads to the average time-dependent velocity

$$\begin{aligned}\langle v\rangle &= \int_{-\pi/a}^{\pi/a}dk\, e^{-\overline{\alpha}(k,t)t}v(k+\mathscr{E}t)\,f(k,0)\\ &\quad+\int_0^t ds\int_{-\pi/a}^{\pi/a}dk\, e^{-\overline{\alpha}(k,s)s}\alpha(k)\,f^{th}(k)\,v(k+\mathscr{E}s).\end{aligned} \tag{105}$$

and, in the steady state, to

$$\langle v\rangle=\int_0^\infty ds\int_{-\pi/a}^{\pi/a}dk\, e^{-\overline{\alpha}(k,s)s}\alpha(k)\,f^{th}(k)\,v(k+\mathscr{E}s). \tag{106}$$

Equation (106) is an exact consequence of the Boltzmann equation in the relaxation time form for arbitrarily $k-$dependent relaxation times [73]. For the constant relaxation time case, $\alpha(k)=\alpha_0=\overline{\alpha}$, one gets

$$\langle v\rangle=\int_0^\infty ds\int_{-\pi/a}^{\pi/a}dk\, e^{-\alpha_0 s}\alpha_0 f^{th}(k)\,v(k+\mathscr{E}s). \tag{107}$$

Explicit evaluation is trivial in the tight-binding limit where $v(k)$ is taken as $v_0\sin ka$, and

$$f^{th}(k)=a\left[2\pi I_0(2V/k_BT)\right]^{-1}\exp(2V\cos ka/k_BT), \tag{108}$$

where I_0 the modified Bessel function, and V the nearest-neighbor transfer integral which is proportional to the bandwidth. One obtains [73, 76]

$$\langle v\rangle=v_0\frac{\mathscr{E}\alpha_0}{\mathscr{E}^2+\alpha_0^2}\frac{I_1(2V/k_BT)}{I_0(2V/k_BT)} \tag{109}$$

showing an Ohmic rise for low fields and negative differential mobility for high fields as in (93), *but no saturation*. An asymptotic analysis presented in [73] shows that such a Boltzmann result can be understood as a relative high temperature consequence of the Fokker-Planck treatment.

Possible Origin of Velocity Saturation

There should be no doubt that, as shown in the previous two sections on the basis of two different methods of analysis, velocity saturation in organic crystals cannot arise as a consequence solely of nonparabolic nature of the carrier bands. Is there anything that can naturally give rise to such saturation? A simple answer has been given recently [74] on the basis of an effective mass equation treatment augmented by Fokker-Planck considerations. The key ingredient necessary in that answer is a $k-$dependent γ in the effective mass equation for the carrier:

$$\hbar\frac{dk}{dt}+\gamma_k v_k = qE. \tag{110}$$

At finite temperatures, we append a noise term to the right hand side of (110) and, through standard procedures, obtain for the evolution of the probability distribution $f(k,t)$ a Fokker-Planck equation

$$\frac{\partial f(k,t)}{\partial t}=\frac{1}{\hbar^2}\frac{\partial}{\partial k}\left[\left(\gamma_k\frac{d\varepsilon_k}{dk}-\hbar qE\right)f(k,t)+\gamma_k k_B T\frac{\partial f(k,t)}{\partial k}\right], \tag{111}$$

which differs from (91) only in the fact that γ_k is here $k-$dependent.

To motivate this suggested mechanism for velocity saturation, start with the Drude equation for the velocity of the carrier,

$$\frac{dv}{dt}+\frac{v}{\tau}=\frac{qE}{m^*}=\frac{qEa}{\hbar}\sqrt{v_0^2-v^2}, \tag{112}$$

where τ is a relaxation time assumed independent of k. We have written the effective mass of the carrier explicitly as $m^*=(1/\hbar)(dv_k/dk)$ *to* obtain the extreme right hand side. Here v_0 is the peak value $2Va/\hbar$ of the velocity in the band assumed sinusoidal for simplicity. From (112), saturation is obtained immediately: at infinite time,

$$v_\infty=\frac{qE\tau}{m^*}=\frac{qE\tau a}{\hbar}\sqrt{v_0^2-v_\infty^2}=v_0\frac{E}{\sqrt{E_c^2+E^2}} \tag{113}$$

where $E_c=\hbar/q\tau a$. The behavior is Ohmic at small fields ($E\ll E_c$) with mobility $\mu_0=v_0/E_c=2Vq\tau(a/\hbar)^2$. The velocity *saturates* for large fields ($E\gg E_c$) to the maximum value $v_0=2Va/\hbar$ that the carrier velocity can have in the band.

What does this mean for the effective mass equation (110) obeyed by the crystal momentum? It is easy to see that to obtain this saturation behavior, the damping coefficient γ_k in (110) must have the *steepness of the effective mass*. Equation (110) gives the same

result as (112) if γ_k is proportional to dv_k/dk. A damping coefficient that is not pathological like m^*, but is nevertheless very steep, will be sufficient to give saturation behavior. Assume an initial occupation by the carrier of a $k-$state at or near the center of the Brillouin zone, and take the $k-$dependence of the damping coefficient to be steep enough so that the carrier, in being accelerated towards the edge of zone, never reaches it, produces no Bloch oscillation, but comes to a steady state. From (110), this will happen when the carrier reaches a $k-$value which satisfies

$$\gamma_k v_k = qE. \tag{114}$$

The steady-state value of the velocity is v_k at that value of k. The field E that produces this velocity equals $1/q$ times the value of $\gamma_k v_k$ at that value of k. The $k-$dependence of γ_k will thus be reflected in the field dependence of the velocity. As a result, the plot of v versus E will show a saturation if γ_k is sufficiently steep: small changes in k will result in large changes in γ_k and thereby of E. In other words, as a consequence of the steepness of γ_k, large changes in the field would be required to produce a discernible change in k and therefore in the velocity. The velocity versus field curve is, thus, essentially the v_k versus $\gamma_k v_k$ curve.

Thus, while saturation does not arise merely from non-parabolic nature of bands, it can arise very simply from steep damping coefficients, at least at zero temperatures. What happens at finite temperatures? From (111), we have

$$f_k = \frac{\int_0^{2\pi/a} dp\, h'_{k+p} e^{\beta\left(\varepsilon_{k+p}-\varepsilon_k\right)} e^{-\beta\hbar qE\left(h_{k+p}-h_k\right)}}{\int_{-\pi/a}^{\pi/a} dk \int_0^{2\pi/a} dp\, h'_{k+p} e^{\beta\left(\varepsilon_{k+p}-\varepsilon_k\right)} e^{-\beta\hbar qE\left(h_{k+p}-h_k\right)}} \tag{115}$$

where a is the lattice constant and

$$h'_k = \frac{dh_k}{dk} = \frac{1}{\gamma_k}. \tag{116}$$

The steady-state velocity is obtained from f_k in (115)

$$v = \int_{-\pi/a}^{\pi/a} v_k f_k dk. \tag{117}$$

Numerical, as well asymptotic, evaluation procedures show [74] that the saturation phenomenon which can be understood for $T = 0$ simply as explained, can persist or be destroyed according to the value of the temperature and the steepness of γ_k. We refer the reader to that analysis [74] for further details, and emphasize here that the essence of the mechanism can be appreciated pictorially by visualizing the manner in which the carrier is stopped in the Brillouin zone by the steep 'wall' presented by γ_k despite the encouragement by the applied field to move in its direction. Perhaps the best way of understanding the mechanism of the velocity saturation of the carrier is in terms of the following modification of Lord Tennyson's well-known charge-related work:

PLIGHT OF THE CHARGE (brigade?)

"I am the carrier," said the hole, "I will not stop."
"Whatever the barrier, I will cross, by flow or hop."

"You forget, you puny charge," replied the wall.
"How steep I rise, above your fields, large or small."
"From this height, I pity your plight, you have much gall."

"Fear not, hole, you ar'n't the sole, wisher of currents."
Said a friendly field, "We will not yield, to scattering tyrants."

Much she tried, the friendly field, to push the hole.
But whatever the p or $\hbar k$, the scattering stole.
Every time, the hole was forced, to the bottom of the bowl.

CONCLUSIONS

If our description of some techniques of modern statistical mechanics in this article has given the appearance of a random walk, we hope it will be regarded to be, at the very least, a *directed* random walk. First, we have examined the memory function formalism and seen how it unifies coherent and incoherent motion, and how it addresses matters as abstract as the origin of irreversibility and topics as concrete as photosynthesis, confined spaces, and granular compaction. Second, we have introduced nonlinear techniques for excitations, mice, and bacteria and investigated selftrapping, epidemic spreads and pattern formation in Petri dishes. Next, we have studied a combination of memory techniques and nonlinear approaches in various juxtapositions: where they blend, coexist, and compete. Finally, we have briefly touched upon kinetic equation approaches and seen how, although 'identical equations have identical solutions' as Richard Feynman is reputed to have said, the same equations can result in very different physics in classical and quantum contexts.

ACKNOWLEDGEMENTS

It is a pleasure to thank my collaborators for the insights they have shared with me about various aspects of science discussed in this article. Singling out only those with whom I have worked within the last year, I thank Guillermo Abramson, Alejandra Aguirre, Alan Bishop, Fred Koster, Jorge Salazar, and Terry Yates regarding the hantavirus and Fisher equations; Maureen Ballard, Miguel Fuentes, Luca Giuggioli, Marcelo Kuperman and Anna Lin, regarding nonlinear evolution with focus on bacteria; and Paul Parris about Fokker-Planck matters. A special vote of thanks is also due to D. Tchawa for his contributions. This research was supported in part by the National Science Foundation grant DMR-0097204 and by a contract made to the Consortium of the Americas for Interdisciplinary Science by Los Alamos National Laboratory.

REFERENCES

1. Morse, P. M., and Feshbach, H., in *Methods of Theoretical Physics* (McGraw-Hill, New York, 1953).
2. See, e.g., *Fundamental Problems in Statistical Mechanics*, ed. E. G. D. Cohen (North-Holland, Amsterdam, 1962).
3. See, e.g., Wu, T. Y., *Kinetic Equations of Gases and Plasmas* (Addison Wesley, 1966).
4. Zwanzig, R. W., in *Lectures in Theoretical Physics* ed. W. Downs and J. Downs (Boulder 1961) Vol. III; in *Quantum Statistical Mechanics* ed. P. H. E. Meijer (Gordon and Breach, New York 1966).
5. Kenkre, V. M., in *Statistical Mechanics and Statistical Methods in Theory and Application* ed. Landman U. (New York, Plenum, 1977).
6. Kenkre, V. M., and Reineker, P., *Exciton Dynamics in Molecular Crystals and Aggregates* (Springer–Verlag, New York, 1982).
7. Kenkre, V. M., *Phys. Rev. E* **18**, 4064 (1978).
8. Kenkre, V. M., and Rahman, T., *Phys. Lett. A* **50**, 170 (1974); see also Kenkre, V. M., *Phys. Rev. B* **12**, 2150 (1975).
9. Kenkre, V. M., Raghavan S., Bishop A. and Salkola M., *Phys. Rev. B* **53**, 5407 (1996).
10. Leggett, A. J. *et al.*, *Rev. Mod. Phys.* **59**, 1 (1987).
11. Kenkre, V. M., and Knox, R. S., *Phys. Rev. Lett.* **33**, 803 (1974).
12. Kenkre, V. M., and Knox, R. S., *Phys Rev B***9**, 5279 (1974); *J. Luminescence* **12**, 187 (1976).
13. Förster, Th., *Ann. Phys. (Leipzig)* **2**, 55 (1948).
14. Salcedo, J., Siegman, A. E., Dlott, D. D., and Fayer, M. D., *Phys. Rev. Lett.* **41**, 131 (1978).
15. Callaghan, P. T., *Principles of Nuclear Magnetic Resonance Microscopy*, (Oxford Univ. Press, Oxford, 1991).
16. Torrey H. C., *Phys. Rev.* **115**, 575 (1959).
17. Sheltraw, D., and Kenkre, V. M., *J. Magn. Reson. A* **122**, 126 (1996); see also Kenkre, V. M., Fukushima, E. and Sheltraw, D., *J. Magn. Reson. A* **128**, 62 (1997).
18. Wang, L. Z., Caprihan, A., and Fukushima, E., *J. Magn. Reson. A* **117**, 209 (1995); see also Caprihan, A., Wang, L. Z., and Fukushima, E., *J. Magn. Reson. A* **118**, 94 (1996).
19. Kenkre, V. M., Scott, J., Pease, E., and Hurd, A. *Phys. Rev. E* **57**, 5841 (1998); Scott, J., Kenkre, V. M., and Hurd, A., *Phys. Rev. E* **57**, 5850 (1998).
20. Kenkre, V. M., *Granular Matter* **3**, 23 (2001).
21. Kenkre, V. M., in "The Granular State", MRS Symp. Proc. Vol. **627**, eds. S. Sen and M.L. Hunt (MRS, Warrendale, PA 2001), pp. 6.5.1-6.5.8.
22. Jaeger, H. M., Nagel,S. R., and Behringer, R. P., *Rev. Mod. Phys.* **68**, 1259 (1996).
23. Train, D., Trans. Instn. Chem. Engrs. **35**, 258 (1957).
24. Aydin, I., Briscoe, B. J., and Sanliturk, K. Y. *Computational Materials Science* **3**, 55 (1994); *Powder Technology* **89**, 239 (1996).
25. Bouchaud, J. P., Cates, M. E., and Claudin, P., *J. Phys. I France* **5**, 639 (1995).
26. Liu, C.-H., Nagel, S. R.,Schecter, D. A., Coppersmith, S. N., Majumdar, S., Narayan, O., and Witten, T. A., *Science* **269**, 513 (1995).
27. Holstein, T., *Ann. Phys.* (N.Y.) **8**, 340 (1959).
28. Kenkre, V. M., in *Singular Behaviour and Nonlinear Dynamics*, eds. St. Pnevmatikos, T. Bountis, and Sp. Pnevmatikos (World Scientific, Singapore, 1989).
29. Kenkre, V. M., *Physica D* **68**, 153 (1993).
30. Brown, D., West, B., and Lindenberg, K., *Phys. Rev. A* **33**, 4110 (1986); see also Kerr, W. C., and Lomdahl, P. S. *Phys. Rev. B* **35**, 3629 (1987).
31. Vitali, D., Allegrini, P., and Grigolini, P., *Chem. Phys.* **180**, 297 (1994) and references therein.
32. Salkola, M., Bishop, A.R., Kenkre,V. M., and Raghavan, S., *Phys. Rev. B* **52**, R3824 (1995).
33. Kenkre, V. M., *J. Luminescence* **76**/**77**, 511 (1998).
34. *Bose-Einstein Condensation*, edited by A. Griffin, D. W. Snoke, and S. Stringari (Cambridge University Press, Cambridge, 1995); see also Milburn, G. J., Corney, J., Wright, E. M., and Walls, D. F., *Phys. Rev. A* **55**, 4318 (1997).
35. Raghavan, S., Smerzi, A., Fantoni, S., and Shenoy, S. R., *Phys. Rev. A* **59**, 620 (1999).
36. Raghavan, S., Smerzi, A., and Kenkre, V.M., *Phys. Rev. A* **60**, R1787 (1999).
37. Kenkre, V. M., and Tsironis. G.P., *Phys. Rev. B* **35**, 1473 (1987).

38. See, for example, *Davydov's Soliton Revisited: Self-Trapping of Vibrational Energy in Protein*, eds. P.L. Christiansen and A.C. Scott (Plenum Press , New York, 1990).
39. Kenkre, V.M., and Wu, H.L., *Phys. Rev. B* **39**, 6907 (1989); see also Kuś, M., and Kenkre, V.M., *Physica D* **79**, 409 (1994).
40. Kenkre, V.M., and Grigolini, P., *Z. Physik* **B90**, 247 (1993); see also Grigolini, P., Wu, H.L., and Kenkre, V.M., *Phys. Rev. B* **40**, 7045 (1989).
41. Kenkre, V.M., and Kuś, M., *Phys. Rev. B* **49**, 5956 (1993); see also Kenkre, V.M., *J. Phys. Chem.* **98**, 7371 (1994).
42. T. Yates *et al.*, *Bioscience* **52**, 989 (2002).
43. Parmenter, C. A., Yates, T. L., Parmenter, R. R., and Dunnum, J. L. *Emerging Infectious Diseases* **5**, 118 (1999).
44. Abramson, G. and Kenkre, V. M., *Phys. Rev. E* **66**, 011912 (2002).
45. Mills, J. N., Yates, T. L., Ksiazek, T. G., Peters, C. J., and Childs, J. E. *Emerging Infectious Diseases* **5**, 95 (1999).
46. Parmenter, C. A., Yates, T., Parmenter, R. R., Mills, J. N., Childs, J. E., Campbell, M. L., Dunnum, J. L., and Milner, J. *J. of Wildlife diseases* **34**, 1 (1998).
47. Abramson, G. and Kenkre, V. M., Proceedings of the Conference on *Unified Science of Technology for Reducing Biological Threats and Countering Terrorism* (BTR 2002), **64,** 312 (2002).
48. Kenkre V. M., unpublished results.
49. Aguirre, M. A., Abramson, G., Bishop, A.R., and Kenkre, V.M., *Phys. Rev. E* **66**, 041908 (2002).
50. Abramson, G., Kenkre, V. M., Yates, T.L., and Parmenter, R., *Bull. Math. Biology*, to be published; see also Abramson, G., elsewhere in these Proceedings.
51. Ben-Jacob, E., Cohen, I., and Levine, H., *Adv. Phys.* **49**, 395-554 (2000).
52. Wakita, J., Komatsu, K., Nakahara, A., Matsuyama, and Matsushita, T M., *Journ. Phys. Soc. Japan* **63**, 1205 (1994).
53. Lacasta, A. M. *et al.*, *Phys. Rev. E* **59**, 7036 (1999).
54. Delprato, A. M., Samadani, A., Kudrolli, A., and Tsimring, L. S., *Phys. Rev. Lett.* **87**, 158102 (2001).
55. Lin, A. L., Mann, B., Torres, G., Lincoln, B., Kas, J., and Swinney, H. L., "Localization and extinction of bacterial populations under inhomogeneous growth conditions", preprint.
56. Nelson, D.R., and Shnerb, N.M., *Phys. Rev. E* **58**,1383 (1998); Dahmen, K.A., Nelson, D.R., and Shnerb, N.M., *J. Math Biology*, **41**,1 (2000).
57. Mann, B., *Spatial phase transitions in bacterial growth*, Ph.D. Thesis (2001), unpublished.
58. Fisher, R.A., Ann. Eugen. London **7**, 355-369 (1937).
59. Anderson, P.W., *Phys. Rev.* **109**, 1492 (1958).
60. Kenkre, V. M. and Kuperman, M. N., "Applicability of the Fisher Equation to the Evolution of Bacteria in a Petri Dish", submitted to *Phys. Rev. E.*
61. Ludwig, D., Aronson, D.G., and Weinberger, H.F. ,*J. Math. Biology* **8**, 217-258 (1979).
62. Giuggioli, L., and Kenkre, V. M., "Analytic Solutions of a Nonlinear Convective Diffusion Equation in Population Dynamics", submitted to *Physica D.*
63. Fuentes, M., Kuperman, M. N., and Kenkre, V. M., "Nonlocal Competition Interactions in Population Dynamics", submitted to *Phys. Rev. E.*
64. Abramson, G. and Kenkre, V. M., *Physica A* **305**, 427 (2002).
65. Manne K., Hurd, A. J., and Kenkre, V. M., *Phys. Rev. E* **61**, 4177 (2000).
66. Abramson, G., Bishop, A.R., and Kenkre, V.M., *Phys. Rev. E* **64**, 066615 (2001).
67. Murray, J. D., *Mathematical Biology* (Springer-Verlag, New York, 1993).
68. Wu, H.L., Kenkre, V. M., *Phys. Rev. B* **39**, 2664 (1989).
69. Kuś, M., and Kenkre, V. M., *Phys. Rev.* **B 45**, 9695(1992).
70. Kenkre, V.M., Skala, L., Weiser, M., and Katz, J.D., *J. Materials Science* **26** (1991) 2483; Kenkre, V. M., *Ceramic Transactions* **21** (1991) 69.
71. Warta, W., and Karl, N., *Phys. Rev. B* **32**, (1985) 1172.
72. Parris, P.E., Kuś, M., and Kenkre, V.M., *Physics Letters A* **289**, 188 (2001).
73. Kenkre, V.M., and Parris, P.E., *Phys. Rev. B* **65**, 205104 (2002).
74. Kenkre, V.M., and Parris, P.E., *Phys. Rev. B* **65**, 245106 (2002).
75. See, e.g., Ziman, J. M., *Electrons and Phonons*, (Oxford University Press, 1960); Dresden, M., Rev. Mod. Phys. bf 33, 265 (1961).
76. Dunlap, D. H., and Kenkre, V. M., *Phys. Rev. B*, **37** (1988).